A Hierarchically Architected Bio-inspired Impact Resistant Natural Fiber Reinforced Composite

Submitted By

Ahsanul Amin

200011111

Mohammad Abraar Hossain

200011146

Supervised By

Prof. Dr. M. Ahsan Habib

A Thesis submitted in partial fulfillment of the requirement for the degree of Bachelor of Science in Mechanical Engineering

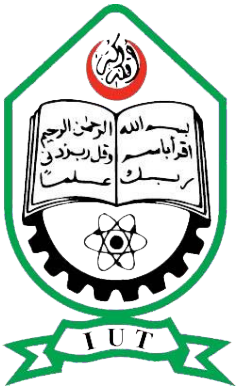

Department of Mechanical and Production Engineering (MPE)

Islamic University of Technology (IUT)

October, 2025

Candidate's Declaration

This is to certify that the work presented in this thesis, titled, "A Hierarchically Architected Bio-inspired Impact Resistant Natural Fiber Reinforced Composite", is the outcome of the investigation and research carried out by me under the supervision of- Prof. Dr. M. Ahsan Habib, Professor, Department of MPE.

It is also declared that neither this thesis nor any part of it has been submitted elsewhere for the award of any degree or diploma.

Ahsanul Amin
Student No: 200011111

Mohammad Abraar Hossain
Student No: 200011146

Recommendation of the Thesis Supervisor

The thesis titled “A Hierarchically Architected Bio-inspired Impact Resistant Natural Fiber Reinforced Composite” submitted by Ahsanul Amin, Student No: 20001111 and Mohammad Abraar Hossain, Student No: 200011146 has been accepted as satisfactory in partial fulfillment of the requirements for the degree of B Sc. in Mechanical Engineering **on 29 September 2025.**

1. ----------
   Prof. Dr. M. Ahsan Habib (Supervisor)
   Professor
   MPE Dept., IUT, Board Bazar, Gazipur-1704, Bangladesh.

CO-PO Mapping of ME 4800 -Theis and Project

COs	Course Outcomes (CO) Statement	(PO)	Addressed by	
CO1	Discover and Locate research problems and illustrate them via figures/tables or projections/ideas through field visit and literature review and determine/Setting aim and objectives of the project/work/research in specific, measurable, achievable, realistic and timeframe manner.	**PO2 Problem analysis**	Thesis Book	
			Performance by research	√
			Presentation and soft skill	
CO2	Design research solutions of the problems towards achieving the objectives and its application. Design systems, components or processes that meets related needs in the field of mechanical engineering	**PO3 Design/development of solutions**	Thesis Book	
			Performance by research	
			Presentation and soft skill	√
CO3	Review, debate, compare and contrast the relevant literature contents. Relevance of this research/study. Methods, tools, and techniques used by past researchers and justification of use of them in this work.	**PO4 Investigation**	Thesis Book	√
			Performance by research	
			Presentation and soft skill	
CO4	Analyse data and exhibit results using tables, diagrams, graphs with their interpretation. Investigate the designed solutions to solve the problems through case study/survey study/experimentation/simulation using modern tools and techniques.	**PO5 Modern tool usage**	Thesis Book	
			Performance by research	√
			Presentation and soft skill	
CO5	Apply moral values and research/professional ethics throughout the work, and justify genuine referencing on sources, and demonstration of own contribution.	**PO8 Ethics**	Thesis Book	
			Performance by research	
			Presentation and soft skill	√
CO6	Perform own self and manage group activities from the beginning to the end of the research/work as a quality work.	**PO9 Individual work and teamwork**	Thesis Book	
			Performance by research	√
			Presentation and soft skill	
CO7	Compile and arrange the work outputs, write the report/thesis, a sample journal paper, and present the work to wider audience using modern communication tools and techniques.	**PO10 Communication**	Thesis Book	√
			Performance by research	
			Presentation and soft skill	
CO8	Recognize the necessity of life-long learning in career development in dynamic real-world situations from the experience of completing this project.	**PO12 Life-long learning**	Thesis Book	
			Performance by research	√
			Presentation and soft skill	

Student Name /ID:

1 Ahsanul Amin 200011111

2 Mohammad Abraar Hossain 200011146

Signature of the Supervisor: ……

Name of the Supervisor: Prof. Dr. M. Ahsan Habib

K-P-A Mapping of ME 4800 -Theis and Project

COs	POs	Related Ks								Related Ps							Related As				
		K1	K2	K3	K4	K5	K6	K7	K8	P1	P2	P3	P4	P5	P6	P7	A1	A2	A3	A4	A5
CO1	PO2	√	√	√	√					√											
CO2	PO3					√				√	√	√				√	√	√	√		
CO3	PO4								√	√	√	√					√	√			
CO4	PO5						√			√				√							
CO5	PO8							√													
CO6	PO9																				
CO7	PO10																				
CO8	PO12																				

Student Name /ID:

1 Mohammad Abraar Hossain 200011146

2. Ahsanul Amin 200011111

3. ……..

Signature of the Supervisor: ……

Name of the Supervisor: ……..

List of Sustainable Development Goals (SDGs) Addressed in this Project

SDG No.	Goals	Targets	Relevance to the Thesis (put √ if valid)	Remarks
1	No Poverty	1.1 Eradicate extreme poverty (people living on less than $1.25/day).		
		1.2 Reduce poverty in all its forms by at least half.		
		1.3 Implement nationally appropriate social protection systems.		
		1.4 Ensure equal rights to economic resources, services, property, inheritance, technology, and financial services.		
		1.5 Build resilience of the poor and reduce exposure to climate-related and other shocks.		
		1.a Mobilize resources to end poverty.		
		1.b Create pro-poor policy frameworks.		
2	Zero Hunger	2.1 End hunger and ensure access to safe, nutritious food year-round.		
		2.2 End all forms of malnutrition.		
		2.3 Double agricultural productivity and incomes of small-scale producers.		
		2.4 Ensure sustainable food production systems and resilient agricultural practices.		
		2.5 Maintain genetic diversity of seeds, plants, and animals.		
		2.a Increase investment in rural infrastructure, research, and technology.		
		2.b Correct and prevent trade restrictions/distortions in global food markets.		
		2.c Adopt measures to ensure proper functioning of food commodity markets.		
3	Good Health and Well-Being	3.1 Reduce global maternal mortality ratio.		
		3.2 End preventable deaths of newborns and under-5 children.		
		3.3 End epidemics of AIDS, tuberculosis, malaria, and neglected tropical diseases.		
		3.4 Reduce premature mortality from NCDs and promote mental health.		
		3.5 Strengthen prevention and treatment of substance abuse.		
		3.6 Halve global deaths/injuries from road traffic accidents.		
		3.7 Ensure universal access to sexual and reproductive healthcare.		
		3.8 Achieve universal health coverage.		

		3.9 Reduce deaths from hazardous chemicals, pollution, and contamination.		
		3.a Strengthen tobacco control (WHO FCTC).		
		3.b Support R&D of vaccines and medicines.		
		3.c Increase health financing and workforce.		
		3.d Strengthen capacity for early warning and risk management.		
4	Quality Education	4.1 Ensure all complete free, equitable, quality primary and secondary education.		
		4.2 Ensure access to quality early childhood development and pre-primary education.		
		4.3 Ensure equal access to affordable technical, vocational, and higher education.		
		4.4 Increase skills for employment and entrepreneurship.		
		4.5 Eliminate gender disparities in education.		
		4.6 Ensure literacy and numeracy for youth and adults.		
		4.7 Ensure learners acquire knowledge/skills for sustainable development.		
		4.a Build and upgrade education facilities that are inclusive and safe.		
		4.b Expand scholarships for developing countries.		
		4.c Increase supply of qualified teachers.		
5	Gender Equality	5.1 End all forms of discrimination against women and girls.		
		5.2 Eliminate violence against women and girls.		
		5.3 Eliminate harmful practices (child, early, forced marriage, FGM).		
		5.4 Recognize and value unpaid care and domestic work.		
		5.5 Ensure women's participation in leadership and decision-making.		
		5.6 Ensure universal access to reproductive health and rights.		
		5.a Undertake reforms to give women equal rights to resources.		
		5.b Enhance use of enabling technology to empower women.		
		5.c Adopt and strengthen policies and laws for gender equality.		
6	Clean Water and Sanitation	6.1 Achieve universal and equitable access to safe drinking water.		
		6.2 Achieve access to adequate sanitation and hygiene.		
		6.3 Improve water quality by reducing pollution.		
		6.4 Increase water-use efficiency and sustainable withdrawals.		

		6.5 Implement integrated water resources management.		
		6.6 Protect and restore water-related ecosystems.		
		6.a Expand international cooperation in water and sanitation.		
		6.b Support participation of local communities.		
7	Affordable and Clean Energy	7.1 Ensure universal access to affordable, reliable, modern energy services.	√	The composite's use of renewable wood fibers supports development of sustainable material technologies aligned with clean energy and green manufacturing.
		7.2 Increase substantially the share of renewable energy.	√	Supports sustainable development of sustainable material technologies aligned with clean energy and green manufacturing.
		7.3 Double global rate of improvement in energy efficiency.		
		7.a Enhance international cooperation on clean energy research/technology.		
		7.b Expand infrastructure and upgrade technology for sustainable energy.		
8	Decent Work and Economic Growth	8.1 Sustain per capita economic growth.		
		8.2 Achieve higher levels of productivity through diversification, tech, and innovation.	√	Promotes sustainable material innovation and efficient production.
		8.3 Promote policies for decent job creation and entrepreneurship.		
		8.4 Improve resource efficiency in production and consumption.	√	Create potential for green jobs and industry diversification.
		8.5 Achieve full and productive employment for all.		
		8.6 Substantially reduce youth not in employment/education/training.		
		8.7 Eradicate forced labour, modern slavery, and child labour.		
		8.8 Protect labour rights and safe working environments.		
		8.9 Promote sustainable tourism.		
		8.a Increase aid for trade support.		

		8.b Develop a global youth employment strategy.		
9	Industry, Innovation, and Infrastructure	9.1 Develop quality, reliable, sustainable infrastructure.		
		9.2 Promote inclusive and sustainable industrialization.		
		9.3 Increase access of SMEs to financial services and integration into value chains.		
		9.4 Upgrade infrastructure for sustainability and resource efficiency.	√	Advances bioinspired engineering and green materials for sustainable infrastructure
		9.5 Enhance scientific research and technology development.	√	Encouraging innovation in composite design and processing.
		9.a Facilitate sustainable infrastructure in developing countries.		
		9.b Support domestic tech development and value addition.		
		9.c Increase access to ICT and internet.		
10	Reduced Inequalities	10.1 Achieve income growth of bottom 40%.		
		10.2 Empower and promote inclusion regardless of status.		
		10.3 Ensure equal opportunity and reduce inequalities of outcome.		
		10.4 Adopt policies for fiscal, wage, and social protection equality.		
		10.5 Improve regulation of global financial markets.		
		10.6 Ensure enhanced representation in global institutions.		
		10.7 Facilitate safe, regular, and responsible migration.		
		10.a Implement special treatment for developing countries.		
		10.b Encourage development assistance and investment in least developed areas.		
		10.c Reduce remittance costs.		
11	Sustainable Cities and Communities	11.1 Ensure access to adequate, safe, and affordable housing.		
		11.2 Provide sustainable transport systems.		
		11.3 Enhance inclusive urbanization and capacity for planning.		
		11.4 Protect cultural and natural heritage.		
		11.5 Reduce disaster impact and losses.		

		11.6 Reduce environmental impact of cities (air quality, waste).		
		11.7 Provide access to safe, inclusive green/public spaces.		
		11.a Support positive links between urban, peri-urban, rural.		
		11.b Increase disaster risk reduction strategies.		
		11.c Support least developed countries in sustainable building.	√	The lightweight, renewable composite has potential for eco-friendly construction materials in sustainable cities.
12	Responsible Consumption and Production	12.1 Implement 10-Year Framework on sustainable consumption/production.		
		12.2 Achieve sustainable management and use of resources.	√	Utilizes renewable wood instead of synthetic fibers
		12.3 Halve per capita global food waste.		
		12.4 Manage chemicals and waste sustainably.		
		12.5 Substantially reduce waste generation.	√	Reducing dependence on non-renewable materials and promoting responsible material cycles
		12.6 Encourage companies to adopt sustainable practices.		
		12.7 Promote sustainable public procurement.		
		12.8 Ensure people have relevant information for sustainable development.		
		12.a Support developing countries' scientific and technological capacity.		
		12.b Develop tools to monitor sustainable tourism impacts.		
		12.c Rationalize inefficient fossil-fuel subsidies.		
13	Climate Action	13.1 Strengthen resilience and adaptive capacity to climate-related hazards.	√	Encourages climate-conscious design
		13.2 Integrate climate measures into national policies.		
		13.3 Improve education and awareness on climate change.	√	Replacing energy-intensive synthetic composites with low-carbon natural alternatives.
		13.a Implement UNFCCC commitments (mobilize $100 billion annually).		

		13.b Promote mechanisms for capacity-building in least developed countries.		
14	Life Below Water	14.1 Reduce marine pollution.		
		14.2 Sustainably manage and protect marine ecosystems.		
		14.3 Minimize and address ocean acidification.		
		14.4 Regulate harvesting and end overfishing.		
		14.5 Conserve at least 10% of coastal and marine areas.		
		14.6 Prohibit harmful fisheries subsidies.		
		14.7 Increase economic benefits from sustainable marine resources.		
		14.a Increase scientific knowledge and marine technology transfer.		
		14.b Provide access for small-scale artisanal fishers.		
		14.c Implement international law for oceans.		
15	Life on Land	15.1 Conserve terrestrial and freshwater ecosystems.		
		15.2 Promote sustainable management of forests.	√	Supports sustainable forestry and wood utilization by promoting *Gmelina arborea*, a fast-growing
		15.3 Combat desertification and restore degraded land.		
		15.4 Ensure conservation of mountain ecosystems.		
		15.5 Take urgent action to reduce biodiversity loss.		
		15.6 Promote fair benefit-sharing from genetic resources.		
		15.7 End poaching and trafficking of protected species.		
		15.8 Prevent introduction of invasive alien species.		
		15.9 Integrate ecosystem values into policies/planning.	√	Usage of renewable species for eco-materials.
		15.a Mobilize resources for biodiversity.		
		15.b Finance sustainable forest management.		
		15.c Support local communities for forest and wildlife.		
16	Peace, Justice and	16.1 Reduce violence and related death rates.		

	Strong Institutions	16.2 End abuse, trafficking, and violence against children.		
		16.3 Promote rules of law and equal access to justice.		
		16.4 Reduce illicit financial/arms flows, organized crime.		
		16.5 Reduce corruption and bribery.		
		16.6 Develop effective, accountable institutions.		
		16.7 Ensure inclusive, participatory decision-making.		
		16.8 Broaden participation of developing countries in global governance.		
		16.9 Provide legal identity for all (including birth registration).		
		16.10 Ensure access to information and protect freedoms.		
		16.a Strengthen national institutions for prevention of violence.		
		16.b Promote/enforce non-discriminatory laws and policies.		
17	Partnerships for the Goals	17.1 Strengthen domestic resource mobilization.		
		17.2 Developed countries to implement ODA commitments.		
		17.3 Mobilize additional financial resources.		
		17.4 Assist developing countries with debt sustainability.		
		17.5 Invest in least developed countries.		
		17.6 Enhance access to science, technology, innovation.	√	Fosters collaboration between academia and industry
		17.7 Promote environmentally sound technologies.	√	Collaboration between academia and industry for sustainable technology development in bioinspired materials
		17.8 Fully operationalize technology bank for LDCs.		
		17.9 Enhance international support for capacity-building.		
		17.10 Promote a universal, rules-based trading system (WTO).		
		17.11 Increase exports of developing countries.		
		17.12 Timely implementation of duty-free, quota-free market access.		

		17.13 Enhance global macroeconomic stability.		
		17.14 Enhance policy coherence for sustainable development.		
		17.15 Respect national policy space.		
		17.16 Enhance global partnerships.		
		17.17 Encourage multi-stakeholder partnerships.		
		17.18 Enhance data capacity of developing countries.		
		17.19 Support capacity-building for sustainable development indicators.		

Acknowledgments

First of all, the authors would like to express gratitude to the Almighty Allah (SWT) for His blessings, which enabled us to complete this thesis successfully. The authors express gratitude to their supervisor Dr. M Ahsan Habib, Professor, Department of Mechanical and Production Engineering (MPE), Islamic University of Technology (IUT), for his continuous guidance, helpful suggestions and supervision at all stages of this thesis work. The authors would also like to express their special gratitude towards Dr. Abu Shaid Sujon, Assistant Professor, Department of Mechanical and Production Engineering (MPE), Islamic University of Technology (IUT) and Dr. Mohammad Nasim, Assistant Professor, Department of Mechanical and Production Engineering (MPE), Islamic University of Technology (IUT) without whom it wouldn't be possible to go through this research work.

Abstract

The Bouligand structure, known for helicoidal fiber alignment in biological materials, offers unique mechanisms for enhancing impact resistance and damage tolerance. This study investigated the mechanical performance of a novel bioinspired composite based on the Bouligand architecture using densified wood (*Gmelina Arborea*) as fiber reinforcement. Composite laminates were fabricated through densification, angular slicing, and epoxy-based lamination to emulate helicoidal layering. The samples were prepared with varying stacking angles and subjected to a comprehensive set of mechanical tests to evaluate their flexural, compressive, impact, shear, and moisture absorption properties. Testing revealed that the composite with the Bouligand structure exhibited significant performance enhancements in multiple domains, whereas anisotropic testing confirmed greater strength in the radial loading directions. The impact strength was approximately 9 times greater than that of untreated wood, which was attributed to energy-dissipative mechanisms such as fiber pull-out and crack deflection. Flexural testing revealed an ultimate strength of 198.22 MPa and a modulus of 27.15 GPa, indicating substantial improvement over conventional stacking configurations. The interlaminar shear strength was highest for the Bouligand configurations, which suggests improved interfacial adhesion due to twisted layering. Microscopic analysis confirmed the role of fiber–matrix interactions and ply orientation in promoting discontinuous crack propagation. Moisture absorption tests revealed enhancements in hydrophobic characteristics. In addition to being lightweight (0.738 g/cm 3), the renewability of fibers demonstrates strong potential for the composite in structural applications, especially in impact-prone or beam structures in transportation or protective panels. This work provides a scalable, bioinspired framework for engineering natural fiber composites with enhanced multifunctional performance, which is a promising alternative to traditional synthetic composites.

Summary

This study was inspired by a natural design found in certain biological structures, where fibers are arranged in a spiral pattern known as the Bouligand structure. This arrangement helps living organisms absorb heavy impacts without breaking. To imitate this, researchers created a new type of eco-friendly composite material using densified wood fibers (from *Gmelina Arborea*) and epoxy resin. The wood fibers were layered at different angles to copy the natural spiral pattern, and the resulting material was tested for strength, flexibility, impact resistance, and water absorption.

The results showed that the bioinspired composite was much stronger and tougher than normal wood—its ability to resist impact was about nine times higher. It also bent and absorbed energy more efficiently because of the twisted fiber layers, which helped stop cracks from spreading. Microscopic observations confirmed that the unique layering improved bonding between fibers and resin, while also making the surface more water-resistant.

Lightweight, renewable, and durable, this new material shows strong promise for use in vehicles, protective panels, and other structures that need to withstand high impacts. The research demonstrates how nature's designs can inspire advanced, sustainable engineering solutions to replace synthetic composites.

Table of Contents

List of Figures

Nomenclatures and Symbol

Symbol	Description
w_f	Weight of the fiber
w_m	Weight of the matrix
w_c	Weight of the composite
ρ_f	Density of the fiber
ρ_m	Density of the matrix
σ_f	Flexural strength (MPa)
E_f	Flexural modulus of elasticity (MPa)
(P)	Applied load (N) or Maximum load before failure (N)
(L)	Support span (mm)
(b)	Width of the specimen (mm)
(d)	Thickness of the specimen (mm)
$\Delta\sigma$	Difference in flexural stress between two selected strain points (MPa)
$\Delta\varepsilon$	Difference between two selected strain points (nominally 0.002)
α_c	Impact strength (J/cm²)
W_c	Energy absorbed during fracture (J)
A	Cross-sectional area (mm²)
σ_c	Compressive stress (MPa)
τ	Interlaminar shear strength (MPa)

Chapter 1: Introduction

The growing demand for sustainable, lightweight, and high-performance materials has accelerated the search for renewable alternatives to conventional synthetic composites. In recent decades, carbon- and glass-fiber-reinforced polymers have dominated the landscape of structural materials owing to their superior mechanical properties. However, the environmental burden associated with their energy-intensive production processes, limited recyclability, and dependence on non-renewable resources has motivated extensive research into eco-friendly substitutes. Natural fiber–reinforced composites have emerged as one of the most promising candidates in this regard, offering renewability, low density, biodegradability, and cost-effectiveness. Nevertheless, their relatively inferior strength, poor interfacial bonding, and high moisture absorption have constrained their widespread adoption in load-bearing applications.

Among the wide range of natural fibers, wood fibers stand out because of their hierarchical microstructure and high specific stiffness. When densified and appropriately treated, wood can exhibit mechanical properties that approach or even exceed those of certain engineered materials. Recent developments in bioinspired design have further unlocked new pathways for enhancing the performance of wood-based composites. Biological structures, such as the Bouligand (helicoidal) architecture found in mantis shrimp dactyl clubs and arthropod exoskeletons, have inspired researchers to mimic nature's toughening strategies. These helicoidally aligned microfibril layers effectively deflect and dissipate cracks, resulting in superior impact and fatigue resistance compared with traditional laminated structures. Translating this concept into engineered wood composites can therefore lead to a new class of bioinspired sustainable materials with outstanding mechanical robustness.[1]

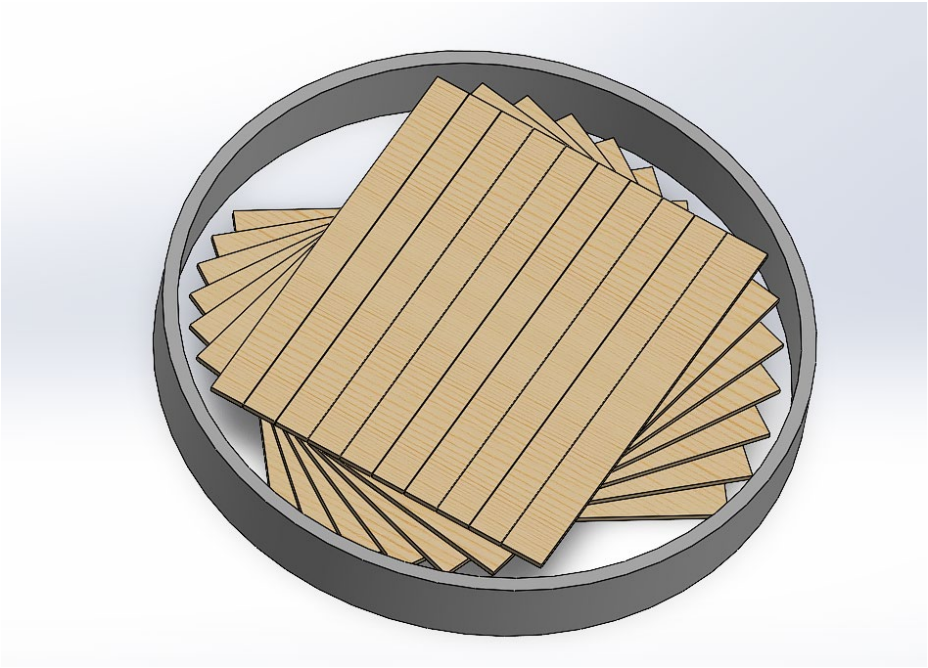

Figure 1: Angular stacking of composite visualized

In this context, the present study focuses on the fabrication and mechanical characterization of densified Gmelina arborea wood fiber composites reinforced with epoxy resin and arranged in a Bouligand-style hierarchical configuration. The choice of *Gmelina arborea* is motivated by its rapid growth, local availability, and favorable fiber morphology, which make it an attractive candidate for sustainable composite development. By densifying the wood fibers and embedding them in an epoxy matrix through controlled compression molding, the material's density and interfacial adhesion are improved significantly. The progressive rotation of fiber orientation between layers—by approximately 16.3° relative to the preceding layer—creates a helicoidal microstructure that mimics the naturally occurring Bouligand pattern. This unique design enables efficient energy dissipation under impact and bending loads while maintaining a lightweight profile.[3]

The objectives of this research are threefold. First, to establish a fabrication route for producing Bouligand-structured wood composites using densified *Gmelina arborea* fibers and epoxy resin. Second, to perform a comprehensive mechanical characterization of the developed composites through flexural, compressive, interlaminar shear, and impact testing according to ASTM standards. Third, to correlate the observed mechanical performance with the underlying microstructural features analyzed via optical and scanning electron microscopy (SEM). By achieving these objectives, the study aims to bridge the gap between sustainable material design and high-performance engineering applications.

The motivation behind this research is rooted in the urgent need to reduce the carbon footprint of structural materials without compromising strength or durability. The densified wood composite developed herein not only leverages renewable resources but also demonstrates a favorable strength-to-weight ratio and energy absorption capacity. The carbon sequestration potential of wood fibers, combined with the relatively low energy required for densification compared with fiber synthesis in synthetic composites, results in a substantially smaller environmental footprint. Consequently, the proposed Bouligand wood composite presents a sustainable alternative for applications such as impact panels, automotive components, and protective gear where both toughness and eco-efficiency are critical.

1.1 Objectives of the Study

- To study the Bouligand architecture and formulate practical methods to replicate this hierarchical structure in engineered composites.
- To apply fiber rotation techniques for simulating the helicoidal arrangement and thereby enhancing the mechanical properties of the reinforced composite.

- To investigate the interfacial bonding behavior between wood fibers and epoxy resin, determining its effect on overall composite performance.
- To analyze the morphological, mechanical, and physical properties of the fabricated composites to assess improvements due to the adopted architecture.
- To examine the anisotropy of the composite material and understand how directional properties influence strength, impact resistance, and failure mechanisms.

1.2 Structure of the Thesis

- Introduction (Background of the study)
- Objectives with specific aims
- Literature review
- Methodology
- Results and analysis
- Conclusion and future scope

Chapter 2: Literature Review

2.1 Introduction

Biologically inspired composites exhibit exceptional strength-to-weight ratios derived from nature's optimized designs. Among these, the Bouligand or helicoidal structure, found in crustaceans like the mantis shrimp, offers outstanding impact resistance through gradual fiber rotation that deflects cracks and dissipates energy. The mantis shrimp's dactyl club, capable of withstanding forces up to 1500 N, exemplifies this efficiency. Meanwhile, densified wood, especially *Gmelina arborea*, provides a renewable, lightweight, and high-strength alternative to synthetic fibers. Its mechanical properties can exceed those of metals and polymers when processed through delignification and thermomechanical compression. This study develops a macroscale Bouligand composite using densified *Gmelina arborea* and epoxy resin through angular slicing and compression molding. Mechanical tests—including flexural, compressive, impact, and shear analyses—were performed to assess performance. The findings demonstrate a sustainable route to high-performance bioinspired composites with potential applications in construction and aerospace.

2.2 Detailed Overview

Biologically inspired composites typically demonstrate enhanced strength–weight ratios materials [1, 2, 3, 4]. In nature, the compositional gradient of structures found in organisms is a product of evolution to meet various needs, i.e., physical protection and predation [5, 6].. Biomimetics involves the fabrication of structures after inspiration from nature. This concept has been applied to modify the design of structural components at the macroscopic level [7, 8].

They have a narrower focus and primarily concentrate on replicating the shape, geometry, or material properties of biological structures to produce a lightweight yet rigid material.

One such accepted biomimetic structure is the helicoidal structure (also popularly known as the Bouligand structure). The Bouligand structure consists of unidirectional fiber-reinforced layers stacked with gradual rotation angle [1, 4, 9], forming a helicoidal pattern resembling the double helix of DNA [9]. These structures are found primarily in arthropods such as stomatopod crustaceans (mantis shrimp club) [10] and arachnids and insects (beetle) cuticle) [1]. Their unique arrangement enhances impact resistance, protecting these organisms against physical damage during high-energy collisions. The helicoidal structure is named after Georges Louis Bouligand, who studied twisted morphologies in various crustaceans, such as arthropod cuticles, ascidian tunica, and dinoflagellate chromosomes, under microscopes. The Bouligand structure found in different animals is crucial for increasing their survival in nature. The highly tolerant structure in those animals can function as a protective material from predators. As a mechanism for defense (crab-shell) [11] or offense (stomatopod club) [5], these biological structures can withstand substantial impact forces, compressive loads, and bending stresses [12]. This structure has also been shown to be stronger than other biomimetics ranges [11]. Bouligand structures exhibit a lower degree of internal damage and greater residual strength than the conventional cross-ply configuration does [11] because of the continual change in the direction of the developing crack caused by the extrinsic toughening mechanism of crack deflection [3][13].

Odontodactylus Scyllarus possesses a specialized raptorial appendage called the “Dactyl”, which resembles a bulbous club [10], that they utilize to capture and consume hard-shelled prey. This club can break through rigid, mineralized structures such as snail shells with

incredible speed (up to 23 m/s) and force [6, 5]. and can exert and withstand forces as high as 1500 N [1]. It can endure cavitation stresses without catastrophic failure [8], exhibiting a distinctive combination of high-speed loading resistance and structural integrity. The club comprises a thick multiphase structure made up of oriented crystalline hydroxyapatite and amorphous calcium phosphate and carbonate, each layer having a comparable 75 μm, separated by protein layers of negligible thickness [3]. This concept can enhance the damage resistance properties for composite fabrication [9].

Although it has structural limitations, wood is a renewable material with a low carbon footprint [14]. By 2100, an additional 106 Gt of CO_2 could be saved if 90% of the population relies on wood for construction [15]. Engineered wood has a hierarchical and porous structure [16]. In addition to being lightweight and structurally rigid, it is ideal for buildings and construction [16, 17]. Additionally, the mechanical properties of wood can be enhanced via delignification [14, 16] and thermomechanical compression [16, 17, 18, 19, 20]. The specific strength of densified wood is superior to that of natural wood. It surpasses many known structural materials, such as plastics, steels, and alloys (the specific tensile strength can exceed that of the Fe-Al-Mn-C alloy [16].). Densified wood can have more than ten times greater mechanical properties than natural wood. For example, Charpy impact tests of densified wood revealed an impact toughness of at least 8.3 times greater than that of natural wood. The flexural strength of densified wood is approximately six times greater than that of natural wood along the growth direction. It is at least 18 times greater perpendicular to it, and its compressive strength is 5.5 times greater along the growth direction, ranging from 33--52 times greater perpendicular to it [14, 18, 21, 22].

Compared with glass fibers and other synthetically produced composites, bio composites require significant improvements, but traditional surface-altering methods can be expensive

[23][24]. Densification because they can be performed at a manageable pressure and temperature, and chemical reactions require minimal temperature control [18]. The use of a stacking sequence, such as this simple method, can increase the optimal strength and toughness and other positive effects such as lower moisture absorption [25][26][27]. The Bouligand stacking sequence has already been proven to have improved. To the best of the authors' knowledge, it has not yet been applied to densified *Gmelina Arborea* [28][29] but has rarely been used for natural fiber-reinforced composites; never before, it has been used for densifying *Gmelina Arborea*, which can be considered a renewable resource compared with synthetic fiber composites, opening doors to greater economic manufacturing possibilities. Another noteworthy point here is that most experiments thus far undertaken to produce Bouligand composites involve the incorporation of nanoparticles or fabrication at a nanoscale [30][31]; the developed composite materials, which can be classified as macroscale composites because of the characteristic size of their reinforcement and matrix phases. Recent studies [32] have been conducted on Bouligand architected concrete, where fracture responses at 25 mm and even 120 mm are studied; as a function of crack length, R-curves are computed to present fracture resistance. Therefore, it is feasible to study the effect of this structure at the millimeter scale.

This paper explores the mechanical properties of a novel bioinspired composite material designed to mimic the helicoidal layering commonly observed in mantis shrimp while using densified *Gmelina Arborea* wood as a natural fiber reinforcement. The composite laminates were subjected to a unique fabrication method involving wood densification, followed by angular slicing, an epoxy-based matrix, and a variation of compression molding. Other variations in ply angles—unidirectional and cross-ply—were also implemented, and the resulting samples were subjected to an extensive array of mechanical tests to assess their flexural, compressive, impact, shear, and moisture absorption characteristics. A high-powered

optical microscope was utilized to study the fracture patterns after testing. The novelty of this study is the fabrication of a macroscale Bouligand structure using densified wood fibers with an epoxy-based matrix. The findings of this study can provide valuable insights into the fabrication of renewable and economical advanced composite materials, contributing to the development of high-performance composites for a wide range of applications, including but not limited to construction and aerospace.

2.3 Key Findings of previous authors

- Biologically inspired composites show superior strength-to-weight ratios and damage tolerance [1–4].
- Bouligand structures with gradual fiber rotation enhance impact resistance and crack deflection [1, 4, 9].
- The mantis shrimp's dactyl club endures impacts up to 23 m/s and 1500 N without failure [1, 5, 6, 10].
- Its layered composition enables energy dissipation and crack arrest under high stress [3, 8].
- Similar helicoidal architectures in arthropods and crustaceans provide bending and compressive strength for protection and predation [5, 11, 12].
- Helicoidal laminates retain higher residual strength and lower internal damage than cross-ply laminates due to crack path deflection [3, 11, 13].
- Wood offers a low-carbon, renewable alternative, potentially reducing >100 Gt CO_2 by 2100 [14, 15].
- Densified wood shows up to 10× improvement in strength and toughness over natural wood [14, 16–22].

- Densification is a simple, cost-effective method for enhancing biocomposite properties [18, 23, 24].
- The Bouligand sequence improves strength and moisture resistance, but is rarely applied to natural fibers and never to densified *Gmelina arborea* [25–29].
- Macroscale Bouligand composites and architectured concretes confirm the structure's scalability and fracture resistance benefits [30–32].

2.4 Topics Addressable in this study

1. No such composites exist that are conventionally fabricated in macro scale for composites
2. Since the impact resistance of bouligand structure can be further enhanced via a engineered biomaterial, here our choice can be densified wood.
3. For binding agent, the comparison of industrial grade resin and protein found in the Mantis Shrimps' Club can be compared.
4. Overall mechanical characterization and comparison with other engineering materials need to be addressed

Chapter 3: Methodology

3.1 Introduction

It was structured to ensure a comprehensive understanding of the relationship between the Bouligand-inspired fiber architecture and the resulting mechanical, physical, and morphological properties of the composite. It begins with the selection and preparation of raw materials, followed by the densification, angular slicing, and lamination processes used to replicate the helicoidal fiber arrangement. The subsequent sections describe the fabrication of test specimens according to relevant ASTM standards and the detailed procedures for mechanical characterization, including Charpy impact, flexural, compressive, and interlaminar shear tests. In addition, microscopic analyses using optical and scanning electron microscopy were conducted to observe fracture behavior and interfacial bonding.

3.2 Preparation of Densified Wood

Wood (*Gmelina Arborea*) blocks with dimensions of 150 mm × 150 mm × 25.4 mm (length × width × thickness) were prepared by cutting in the longitudinal direction via a table saw. The blocks were then oven-dried for 1 hour at 103°C to de-moisturize them [33]. Figure 1 illustrates the overall workflow of this study, indicating the preparation of wood composite samples for conducting different mechanical tests. Afterwards, the samples were placed into a 5 L beaker. A solution of sodium hydroxide (2.5 M NaOH) and sodium sulfite (0.4 M Na_2SO_3) was prepared [14][34]. The bulk wood pieces were fully submerged for 24 hours at 65°C [35] in this solution, and the beaker was kept on a heating mantle at a constant temperature, resulting in the delignification process [14][22].

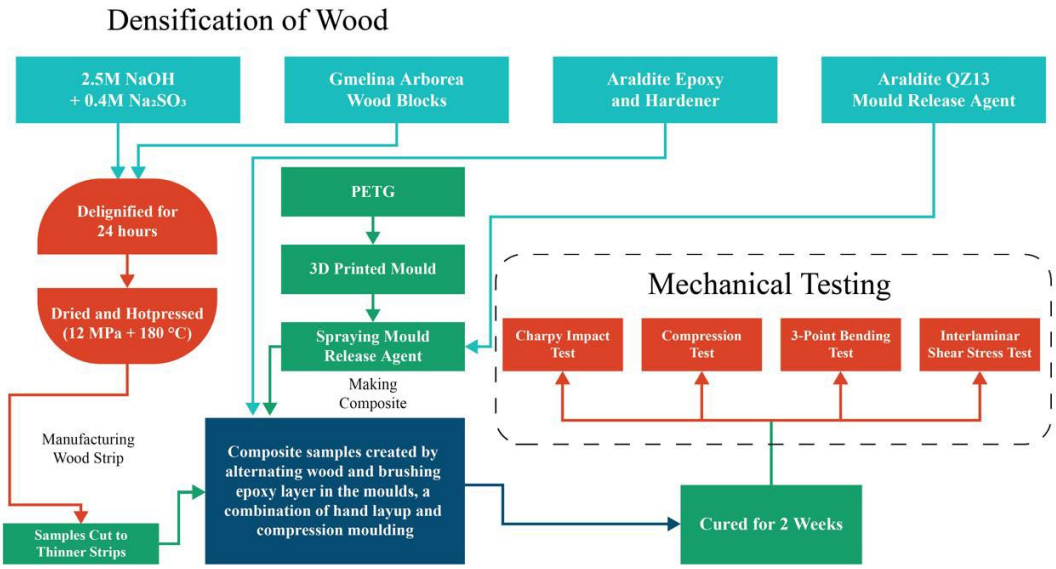

Figure 2: Overview of the study workflow

Wood lignin reacts with sodium hydroxide (NaOH) and sodium sulfite (Na_2SO_3), where sulfide ions attack the ether bonds, breaking the lignin into soluble phenolic compounds (Ar-OH). The sulfite process uses sulfur dioxide (SO_2) and sulfite/bisulfite ions (HSO_3^-) under acidic or neutral conditions to sulfonate lignin. This phenomenon makes lignin more water-soluble. The color of the solution gradually changed to dark brown [14].. The treated wood sample was then repeatedly washed seven times in a warm water solution of acetic acid to remove any remaining sodium hydroxide [36][37][34][22].

The treated wood samples were thermo-mechanically pressed under a pressure of 12 Mpa at a constant temperature of 180°C in a controlled environment maintaining 40% humidity perpendicular to the wood growth direction [18] via a CARVER 38914NE100 USA hot-press machine. A stainless-steel mold was designed and fabricated to maintain dimensional stability during the hot-pressing process (without the mould, one of the trial samples expanded in the radial direction by 14 mm). The thickness of the wood decreased by 60%, resulting in proper densification. To produce one densified wood sample, 1 hour of heated pressing was followed by 1 hour of pressure maintenance while the coolant was flown within the plates. The final

densified wood blocks-maintained dimensions of 150 mm × 150 mm (length × width), and the thickness was reduced to 10 mm.

3.3 Testing Sample Preparation

Figure 3: Sample of the composite material exhibiting angular variations under display.

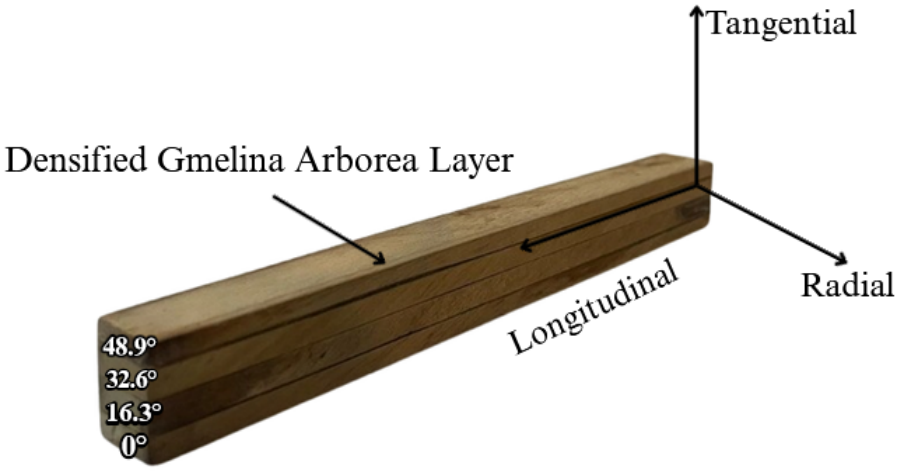

Figure 4: Axes Orientation of the Densified Wood Composite

The densified wood samples were cut into thin strips via CNC milling. The dimensions of each strip were 10 mm (radial) × 150 mm (longitudinal) × Mm (tangential). The cuts were performed in an angular fashion, where the rotation of the fiber was maintained over the z axis (tangential axis), and the rotations were 0°, 16.3°, 32.6°, and 48.9° because an increment of 16.3° resulted in superior mechanical properties according to the literature [11].

The goal was to stack the strips one on top of the other in ascending order of their angles. A 1:1 mixture (by volume) of Araldite AW 106 resin and HARDENER HV 953 IN was used as a binding agent. Another mould was subsequently 3D printed with polyethylene terephthalate glycol (PETG) to increase the dimensional stability of the composite laminate while curing. Araldite QZ13 mould release agent was sprayed on the walls. After a thin epoxy coating was applied on the bottom, the strips were placed, and the epoxy resin was brushed between layers. The moulds were joined via nuts and bolts to provide compression during the curing stage, so any trapped air bubbles escaped the epoxy, and the bonding strength was increased. (Figure2b) [38] Samples were prepared at the convenience of testing (Figure 3a and 3b), which is mentioned in the next subsection.

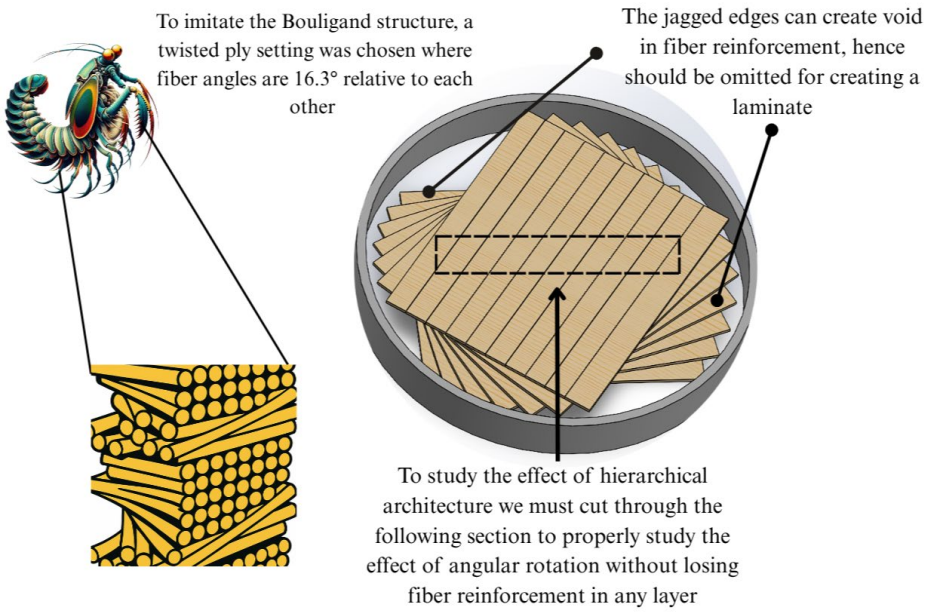

(a)

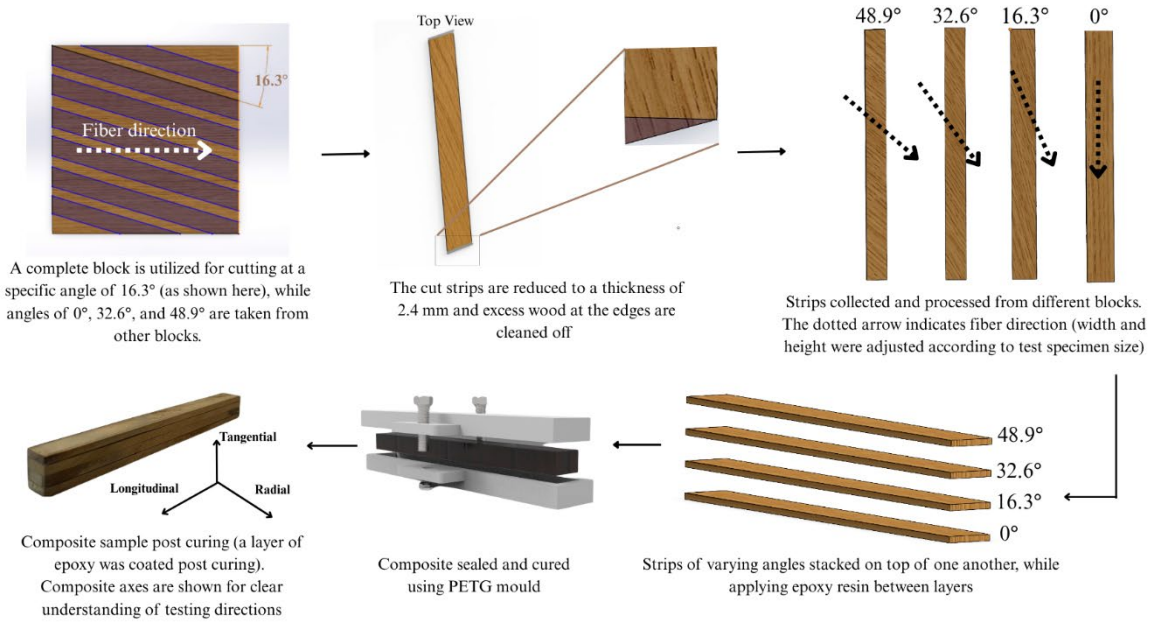

(b)

Figure 5: (a) Design motivation of fabricating Bouligand wood composite and (b) the composite fabrication process

3.4 Weight and Volume fraction of the fibers and composite

The weights of the composite and wood fibers were measured via an electronic weight balance in a closed environment. The composite density and fiber density were subsequently measured via a pycnometer. The following formulas were used to calculate the weight fraction and volume fraction. The fiber weight fraction and volume fraction in a composite is given by (1) and (2):

$$w_l = \frac{w_f}{w_c} \tag{1}$$

$$v_f = \frac{\frac{w_f}{\rho_f}}{\frac{w_f}{\rho_f} + \frac{w_m}{\rho_m}} \tag{2}$$

3.5 Morphological Properties

Morphological properties, including the microstructure and fracture behavior of the Bouligand composite samples after mechanical testing, were analyzed via a Euromex iScope IS.1153-EPL high-powered optical microscope. Samples from mechanically tested Bouligand composites were prepared and observed. A range of magnifications from 60x to 150x was employed, with lower magnifications used to study the crack angles and higher magnifications utilized to examine fracture angles. Morphological characteristics such as particle dispersion, were examined using a TESCAN VEGA 3 High-Performance Scanning Electron Microscope (TESCAN, Brno, Czech Republic) operated at an accelerating voltage of 15 kV. Samples were sputter-coated with a thin layer of gold to minimize charging effects.

ImageJ (open-source image processing and analysis software) was used to count the pixels of

the images and calculate the scale of each micrograph [39].

3.6 Study of Anisotropic Properties

Wood is generally an anisotropic material, meaning that its mechanical properties vary significantly in the transverse, radial, and longitudinal directions. This anisotropy arises from the complex cellular structure of wood, including features such as tracheid, vessels, rays, and annual rings. Wood has a maximum strength and stiffness parallel to the grain and a minimum strength and stiffness perpendicular to the grain. Hence, timber structures are generally discouraged from being made in a perpendicular direction [40] [41].

Compared with those in the matrix, fibers are the primary load-bearing constituents in composites because of their superior stiffness and strength. When fibers are aligned with the direction of applied stress, they facilitate efficient load transfer, resulting in increased tensile strength and stiffness.

Alternatively, misalignment between the fiber orientation and stress direction compels the load to traverse through the more compliant matrix, which is the path of least resistance, leading to diminished mechanical performance [42].

3.7 Tests conducted

3.7.1 Flexural Test

For the flexural test, the dimensions of the samples were taken as 150 mm × 10 mm × 10 mm (length × width × thickness). Samples of untreated wood, densified wood, straight composite, and Bouligand composite were cut according to ASTM D143[43][44].. The samples were placed in a PLS100 Universal Testing Machine (Jinan Testing Equipment IE Co. Ltd.,

Shandong, China). The cross-head speed was 1 mm/min. The span length for the test setup was kept constant at 60 mm, with an average span-to-thickness ratio of 15, and tests were performed, with the samples resting on two fixed supports. A loading pin was applied to the sample with a controlled force until the first sign of failure was observed. The flexural strength is calculated via equation (3):

The flexural modulus and strength is calculated via equation (3) and (4):

$$\sigma_f = \frac{3PL}{2bd^2} \tag{3}$$

$$E_f = \frac{\Delta\sigma}{\Delta\varepsilon} \tag{4}$$

3.7.2 Charpy Impact Test

The impact strength was measured quantitatively via the Charpy impact test. Samples of untreated wood, densified wood, straight composite, and Bouligand composites were prepared, measuring 55 mm × 10 mm × 10 mm (length × width × thickness). The Charpy test was conducted via an AIT-300-N impact testing machine. The Charpy impact strength is calculated via equation (5):

$$\alpha_c = \frac{W_c}{A} \tag{5}$$

3.7.3 Compression Test

For the static compression test, sample sizes of 30 mm × 20 mm × 20 mm (length × width × thickness) were created for each sample (untreated wood, densified wood, straight composite, and Bouligand composite) and placed in the hydraulic press of the PLS100 Universal Testing Machine [43][44]. A controlled compressive force was applied at the center via a hydraulic press, and the load was increased until failure was observed. The compressive stress is given

by (6):

$$\sigma_c = \frac{P}{A} \tag{6}$$

3.7.4 Short Beam Shear Test

The interlaminar shear strength is an excellent method for quantitative measuring the adhesion capabilities of the layers within a structure. According to recent literature, the Short Beam Shear (SBS) test can be an excellent tool for measuring this phenomenon [45, 46]. Short beam shear test sample sizes of 42.5 mm × 10 mm × 10 mm were made after following the ASTM D2344 standard and using a PLS100 Universal Testing machine (Jinan Testing Equipment IE Co. Ltd., Shandong, China). The testing was performed according to the specified standard via a 3-point bending setup with a 1 mm/min crosshead speed. The crosshead movement was stopped when the deflection of the beam exceeded the nominal thickness of the sample. The test was conducted after ensuring proper alignment on the support spans. interlaminar shear strength (ILSS) is given by (7):

$$\tau = \frac{0.75P}{bd} \tag{7}$$

3.7.5 Moisture Absorption Test

Samples measuring 50 mm × 50 mm were used for the moisture absorption test. The samples were immersed in water at an ambient temperature of 24°C, and their mass was recorded over 21 days. The moisture absorption percentage was calculated via the following equation (8):

$$\text{Moisture Absorption (\%)} = \frac{m_2 - m_1}{m_1} \times 100 \tag{8}$$

3.8 Chapter conclusion

In summary, the methodological framework employed to develop and evaluate the bioinspired densified wood fiber composite. A step-by-step procedure was designed to ensure precision in material selection, processing, and testing, beginning with the preparation and densification of *Gmelina Arborea* wood fibers and continuing through angular slicing, lamination, and specimen fabrication. The use of standardized testing methods enabled accurate assessment of the mechanical, physical, and morphological properties, while microscopy provided insight into fracture mechanisms and fiber–matrix interactions. Moisture absorption and carbon-footprint analyses were also incorporated to evaluate the composite's environmental durability and sustainability. Collectively, these procedures established a rigorous and reproducible foundation for validating the performance of the developed Bouligand-inspired composite, forming the basis for the experimental results and discussions presented in the next chapter.

Chapter 4: Results and Discussions

4.1 Chapter Introduction

This chapter presents and interprets the experimental findings obtained from the mechanical, physical, and morphological analyses of the developed Bouligand-inspired densified wood fiber composite. The results are systematically discussed to establish the relationship between the helicoidal fiber arrangement and the enhanced mechanical performance of the composite material. Each section highlights the effects of fiber orientation, layer stacking sequence, and densification on parameters such as flexural strength, impact energy absorption, interlaminar shear strength, and compressive behavior. Microscopic observations, including optical and scanning electron microscopy, are used to interpret the failure mechanisms and validate the role of the Bouligand architecture in improving crack deflection, fiber pull-out, and interfacial bonding. Furthermore, the chapter analyzes the composite's anisotropic characteristics, moisture absorption trends, and production-stage carbon footprint, comparing them with conventional materials to emphasize its multifunctional and sustainable performance. The fabricated materials properties were compared with other engineering materials to assess the applicability in various structural and impact prone applications.

4.2 Analysis of the study

4.2.1 Morphological Studies

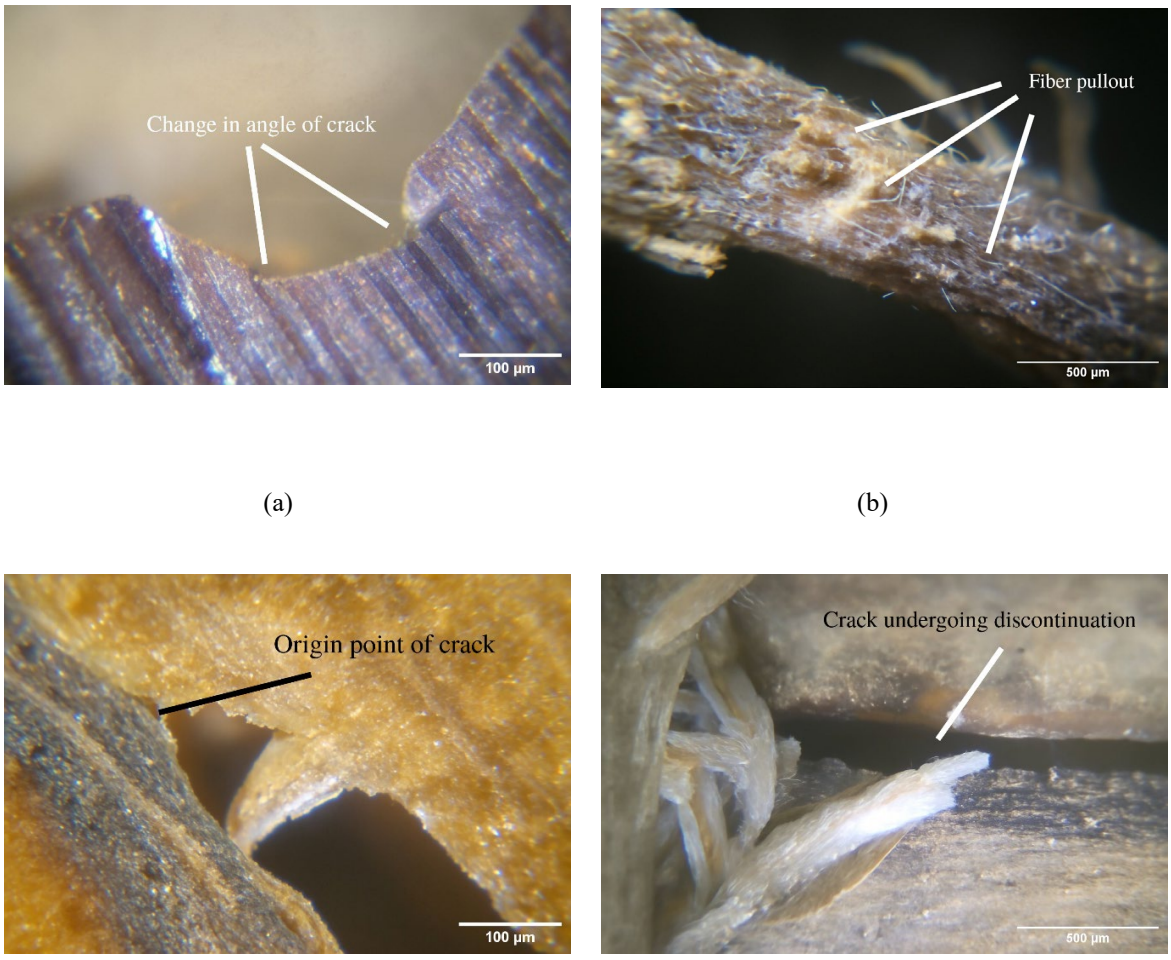

Figure 6: Microscopic Image of (a) Crack Surface of Charpy Sample (b) Fiber Debonding (c) 3 point bending sample crack origin (d) Propagation of same crack

The interface between the fiber and matrix plays a crucial role in crack deflection. A strong bond may lead to fiber breakage or pull-out, whereas a weak bond can cause debonding, altering the crack's trajectory. This interaction can cause the crack to deviate from its original path, leading to a more tortuous crack path [47]. A substantial amount of crack propagation and delamination can be observed in the micrographs taken under a high-powered microscope.

Figure 4a and Figure 4b are from a Charpy test sample of the Bouligand composite. Figure 4b shows that fiber pullout has occurred. Since natural fibers such as wood can be ductile, they do not break easily under impact. Instead, they may often be pulled out from the matrix while remaining intact [48]. These debonded fibers absorb energy effectively, slowing down cracks present [49].

Figure. 4a is taken from the surface of a composite sample that has broken in two because of the Charpy test. The angular variation of the crack is noticeable; this could be due to either of two reasons: fracture toughness, as the fracture toughness of wood and epoxy are different. Wood may exhibit more resistance to crack initiation in some directions, such as along the grain, whereas epoxy has a lower fracture toughness. The other reason could be that differences in material properties can change the crack angle as the crack encounters various resistances from each material [50].

In Figure 4c, which is taken from a Bouligand composite that underwent the 3-point bending test, it is evident that the crack originated from a point possibly between the interface of the fiber and the matrix. The crack seems to follow a path of least resistance, propagating through the material and appearing to cut across the fiber alignment. Figure 4d, taken from the same sample shows the continuation of the crack observed in Figure 4c, and it becomes discontinuous after a while. This occurred most likely because the crack encountered an interface of fiber and matrix, deflecting from its original path and taking a more tortuous form [51].

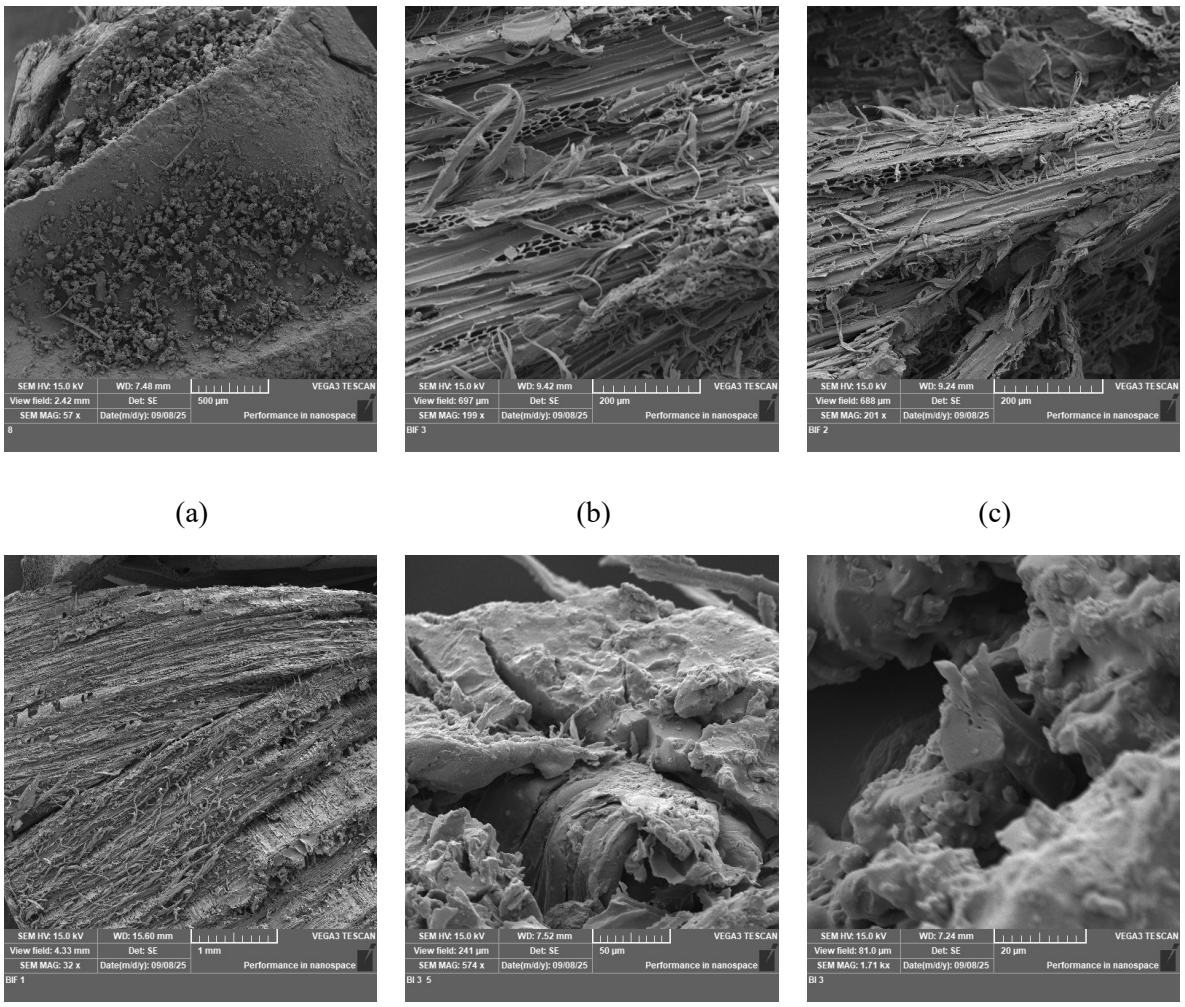

(a) (b) (c)

(d) (e) (f)

Figure 7: Scanning Electron Microscopy of Charpy sample of Bouligand composite: (a) Change in crack angle observed same as Figure 4a, (b) Collapsed cellular lumens in the densified wood specimen, (c)Fiber debonding and pullout observed, (d) Top perspective of the angular orientation (e) Untreated tubule of the structure (f) Epoxy accumulation at crack site.

Figure 5 presents the Scanning Electron Microscopy (SEM) analysis of a Charpy-tested Bouligand composite, revealing a series of critical microstructural features that contribute to its fracture resistance and overall performance. In **Figure 5a**, a distinct change in crack propagation angle is observed, consistent with the trend identified in Figure 4a, which highlights the influence of helicoidal fiber alignment on deflecting cracks away from their

initial path**. Figure 5b** displays collapsed cellular lumens within the densified wood specimen, a consequence of the compression process that eliminates porosity and enhances load-bearing capacity. This structural densification reduces weak points within the composite, thereby improving its resistance to crack initiation and propagation. In **Figure 5c**, evidence of fiber debonding and pullout is visible, a mechanism often associated with energy dissipation during fracture. This phenomenon demonstrates how fiber–matrix interactions act as a secondary toughening mechanism by absorbing fracture energy and delaying catastrophic failure [48].

Further observations highlight additional microstructural mechanisms that reinforce the Bouligand architecture. **Figure 5d** shows a top perspective of the sample, clearly illustrating the angular stacking between successive layers. This helicoidal orientation not only alters crack trajectories but also distributes stress across multiple planes, thereby enhancing toughness. **Figure 5e** presents an untreated region of the composite characterized by vacuoles and intact lumens, in contrast to the densified zones. These untreated regions underscore the significance of densification in strengthening the material while also providing a baseline for comparison. Finally, **Figure 5f** depicts a discontinuation of crack propagation, consistent with the phenomenon illustrated in Figure 4d [47]. Such discontinuities indicate effective crack arrest, confirming that the Bouligand-inspired design provides a synergistic combination of crack deflection, fiber pullout, and interlayer orientation to achieve superior fracture resistance [51].

4.2.2 Anisotropic Properties of the composite

The 3-point bending tests conducted in different loading directions produced drastically different properties, as shown in Figure 6a. The loaded surface for the radially loaded sample has alternating layers of fibers and matrix, whereas the loaded surface for the tangentially loaded sample is purely fibrous. The ultimate strength was substantially lower for the

tangentially loaded sample, which was 120.06 MPa. This is a 39.16% decrease from the ultimate strength of the radially loaded Bouligand sample. This finding supports the literature regarding different loading directions for wood, where radial strength loading is greater [59].

Figure 6b shows the compressive strength of the Bouligand wood composites under various loading orientations. Figure 6b clearly shows that in both the tangential and longitudinal orientations, the samples did not experience sudden failure but rather a slight downward trend in the stress–strain graph. However, there was no secondary phase of stress increase, with only one peak, and it underwent crushing. The specimens loaded in the longitudinal direction exhibited a lower ultimate strength (11.93 MPa) than those loaded in the other directions because individual fiber buckling is accompanied by layer buckling. In the tangential sample, the top layer failed at the ultimate point, and different layers could not support further stress, resulting in complete failure. The failure is nearly at 0.3% strain; hence, this load in this orientation makes the sample very sensitive to first-ply failure.

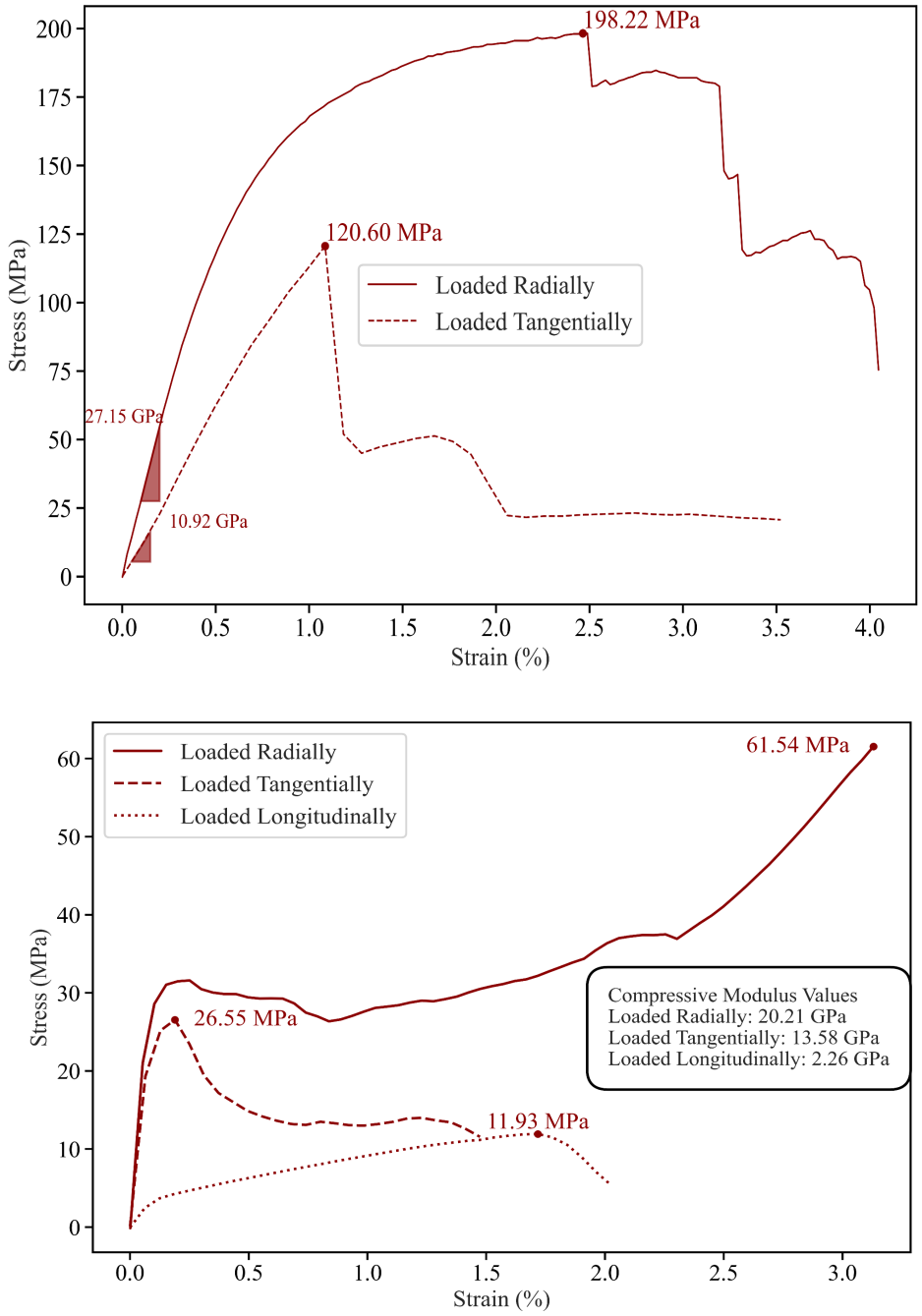

Figure 8: (a) Comparison of (a) flexural strength, (b) compressive strength of the Bouligand wood composite samples loaded in different orientations

4.2.3 Impact Properties

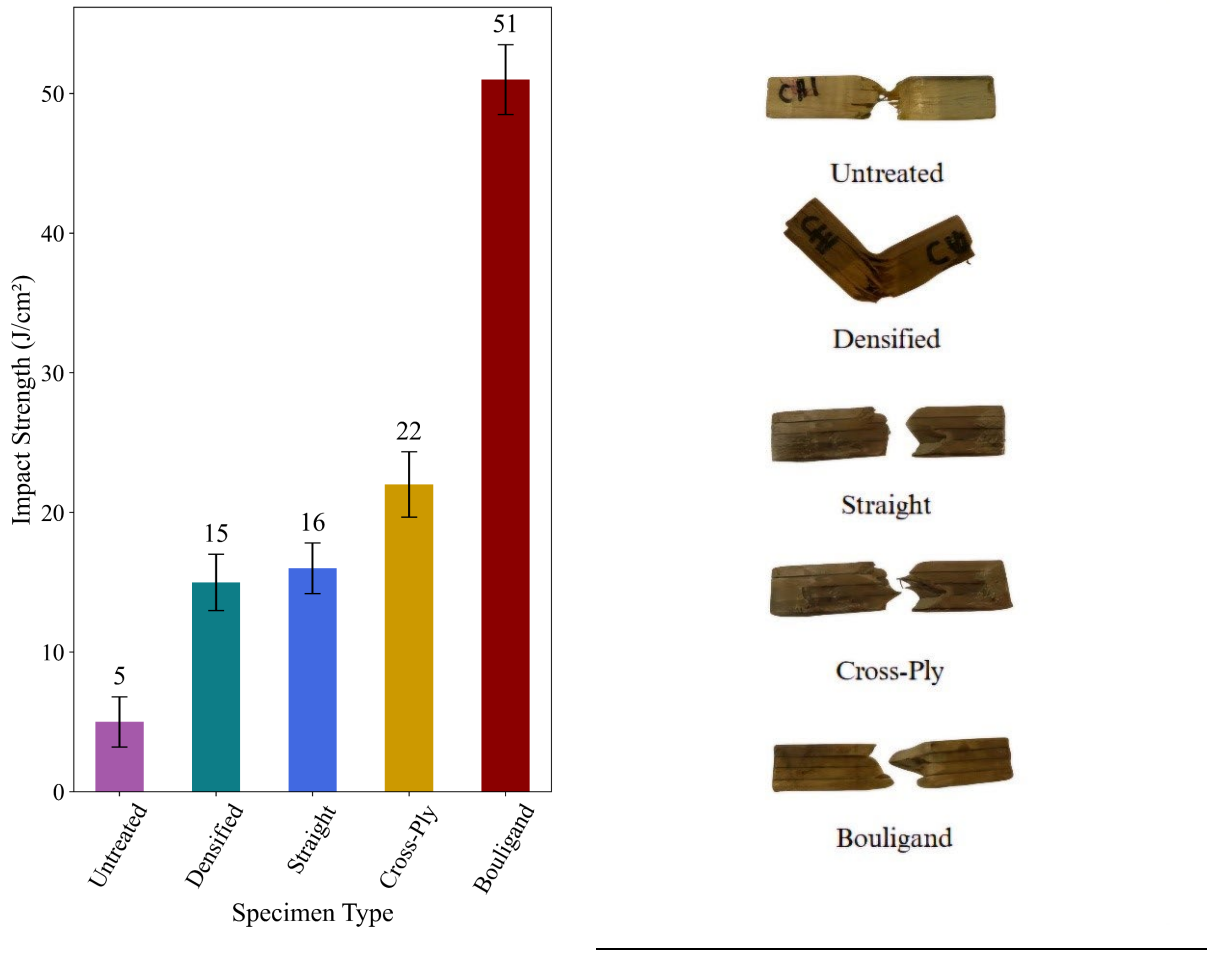

Figure 9: (a) Impact Energy of different wood specimens and (b) typical fracture outcomes of specimens after Charpy impact testing

The study of impact properties is the main highlight of the Bouligand structure. This property demonstrated the most significant improvement in this study, which is consistent with previous studies. Furthermore, a low-velocity impact test was used to illustrate the dominant failure mode exhibited by a twisted ply structure at both the micro- and macro-scale. Three samples were tested for each case, and the average impact strengths are plotted in the Figure. 7a. Bouligand structure combined with the densification process has resulted in an almost 9-fold increase in impact strength, as shown in Figure 7a. The densification process alone has resulted

in almost 3 times the impact strength, which supports the previous study [18]. Adding epoxy within layers of unidirectional stacked densified wood (UD sample) has not led to significant changes in impact properties over solid densified wood (DW). However, the impact strength significantly improves when the fibers are oriented at a continuous increment of angles (Bouligand).

Importantly, unlike other mechanical tests, the primary failure mode observed in the Charpy test was fiber failure. The instantaneous load results in a combination of fiber debonding and fiber cracking. The crack propagation was discontinuous between layers in the Bouligand structure, contrary to the continuous propagation in the UD structure. Therefore, rotation of the ply causes a complex path for the crack to propagate [1], improving the impact absorption capability.

4.2.4 Flexural Properties

The failure mode of the samples was a combination of fiber failure and layer delamination. Unlike the dynamic bending observed in the Charpy test, the quasistatic bending caused significant delamination in the outer layers of the composite.

An increase in both the ductility and toughness of the wood sample was observed in the densified sample compared with the untreated wood sample, as per Figure 8a. Compared with the maximum stress of 84.38 MPa for the untreated sample occurring at 1.37%, the failure strain criterion is consistent with previous studies [52]. The densified sample shows an improvement with an ultimate strength of 138.15 MPa at 2.75%. This is due to the reduced volume of the tubular fibers in the wood [17, 18] due to densification, which has caused tight

packing of the fibers, resulting in a more ductile response [34]. The addition of epoxy layers between the fibers has converted the material's characteristics to brittle, as the ultimate failure point has shifted to a lower strain value of 1.64% in the UD sample. However, the ultimate strength slightly improved to 150.97 MPa. This is because epoxy resin is a brittle material [53], and reinforcement with comparatively ductile fibrous material can enhance its properties [54]. Adding epoxy also moves the neutral axis, resulting in an increase in bending properties [22]., a change in the orientation of the fibers, and an increase in ultimate strength of 160.20 MPa per Figure 8a. The best results were obtained for the Bouligand composite in accordance with the Charpy results discussed previously. The tests indicate that the ultimate strength of the Bouligand sample is 198.22 MPa at a strain of 2.46%.. A special characteristic of the Bouligand graph is a step-down reduction in the stress values by 90 degrees (cross-ply), which does not change the strain value from the UD orientation. In contrast, the other graphs show a two-step reduction accompanied by a sudden drop in the stress value. Therefore, the Bouligand structure on a macroscopic scale for fiber-reinforced composites can significantly improve their toughness.

A linear regression model was applied to the stress–strain data to obtain the flexural modulus. The data obtained are plotted in Figure 7e. and suggest that the densification process improved the stiffness of the material. The flexural modulus increased from 13.03 GPa for untreated wood to 22.84 GPa for densified wood, representing a substantial improvement. However, adding brittle matrix material yielded minimal benefit (22.33 GPa), and the cross-ply structure exhibited a lower modulus (16.12 GPa), although it was still greater than that of the untreated sample. Consistent with the previous improvements, the flexural modulus obtained for the Bouligand structure was the highest, reaching 27.15 GPa.

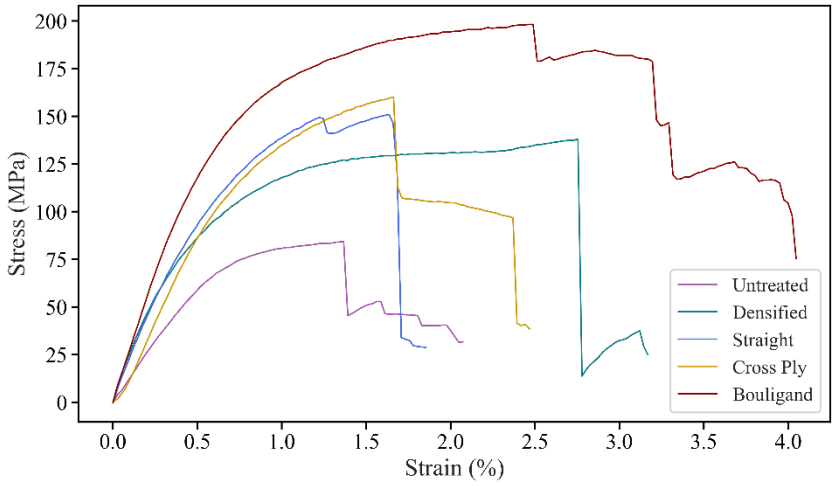

(a)

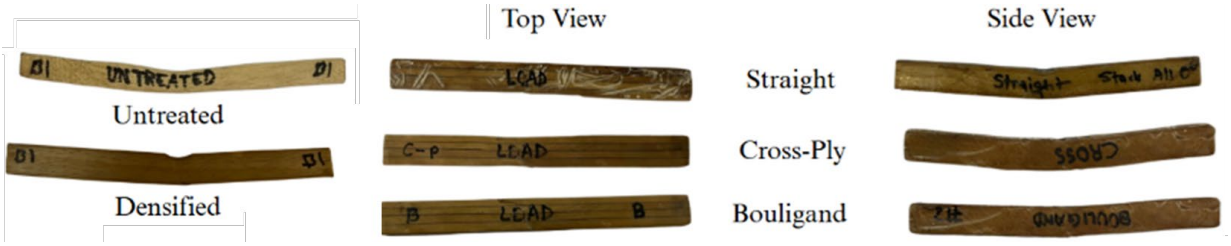

(b)

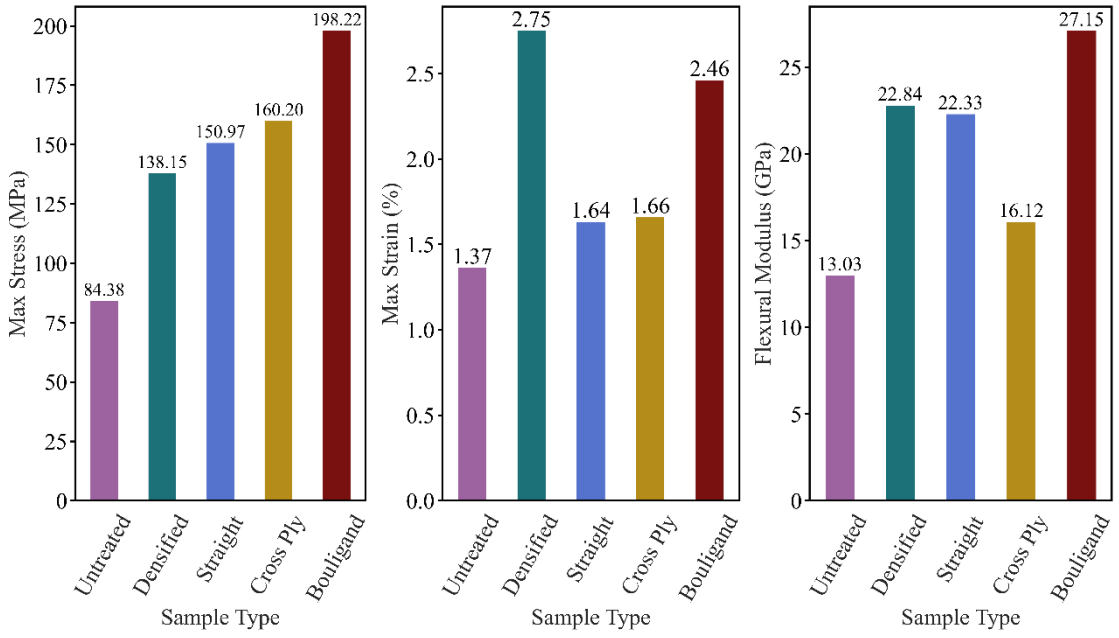

(c) (d) (e)

Figure 10: (a) Comparison of stress-strain curves obtained during flexural tests, (b) condition of different samples after flexural testing, (c) ultimate flexural strength, (d) flexural strain value observed at ultimate failure point, (e) flexural Modulus

4.2.5 Compression Properties

In Figure 8a,, the curves for untreated wood and densified wood show a similar trend, where the samples first exhibit an elastic region, then a plateau region, and finally a densification region. However, in the end, it ultimately fails catastrophically. From the similarity in the characteristics of the untreated and treated wood samples, delignification clearly increased the capacity of the samples to undergo more compression. Additionally, the pressure of 12 MPa during the hot-pressing stage is very well below the failure point of 111.64 MPa for treated wood, and the blocks could be compressed with higher loads to achieve a greater reduction in thickness. The height of the sample was reduced from 30 mm to 11 mm during this process, and ultimately, the densified sample experienced catastrophic failure.

However, in the composite, although the value of the ultimate strength under compression decreased instead of causing catastrophic failure, the first peak of the stress–strain graph indicates the point after which delamination occurred and the fibers started to debond. However, the composite does not fail immediately; instead, it deforms much more while maintaining a near-constant stress value similar to the plateau region. At a strain rate of nearly 2%, all the samples exhibit an exponential increase in stress and fail catastrophically. The samples seemed to buckle individual fiber layers, and the bouligand samples performed worse (61.54 MPa) than the nearly identical values for the straight (69.24 MPa) and cross-ply (73.08 MPa) structures but allowed a greater degree of deformation. Surprisingly, in Figure 8e, although there is a decrease in strength, the linear regression model suggests that the compressive stiffness increases significantly up to 16.66 GPa for the straight orientation and approximately 20 GPa for both the cross-ply and the Bouligand structure.

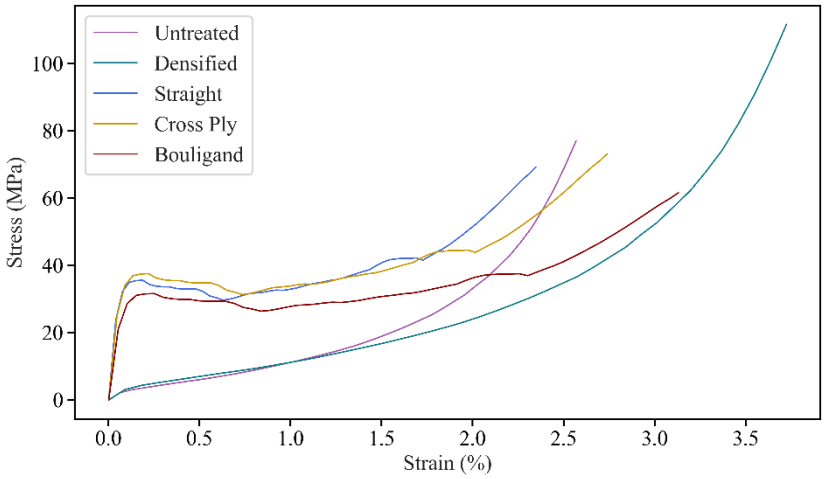

(a)

(b)

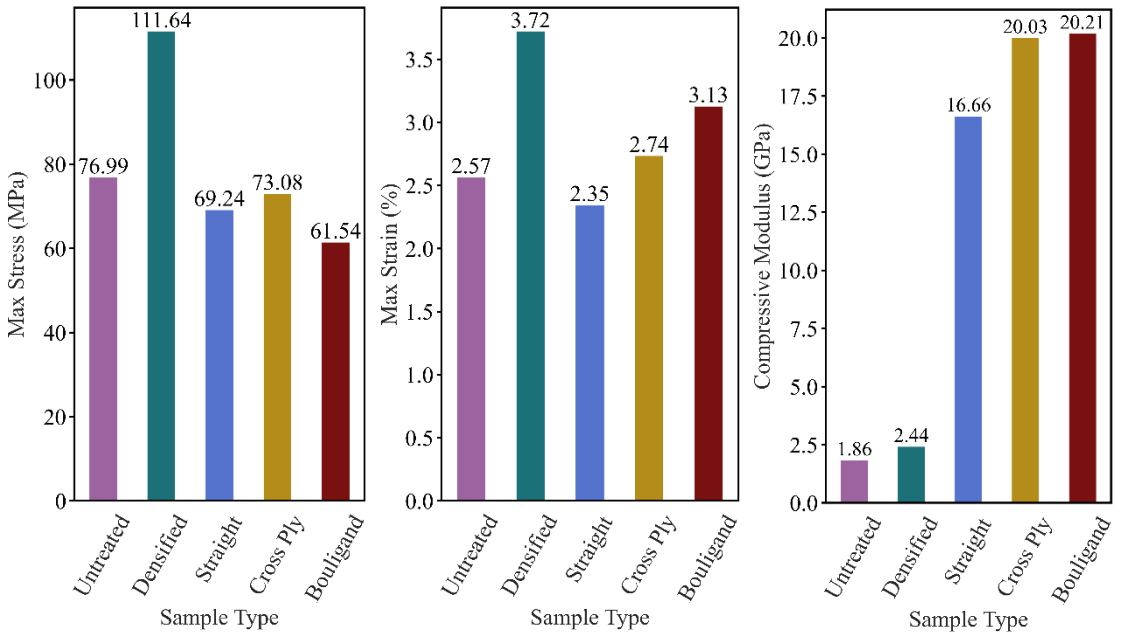

(c) (d) (e)

Figure 11: (a) Comparison of Stress-strain curves exhibited in compressive tests loaded in radial direction, (b) condition of different samples after quasi-static compression testing, and (c) ultimate compressive strength, (d) compressive strain value observed (e) Compressive modulus observed in radial direction

4.2.6 Interlaminar Shear Strength (ILSS)

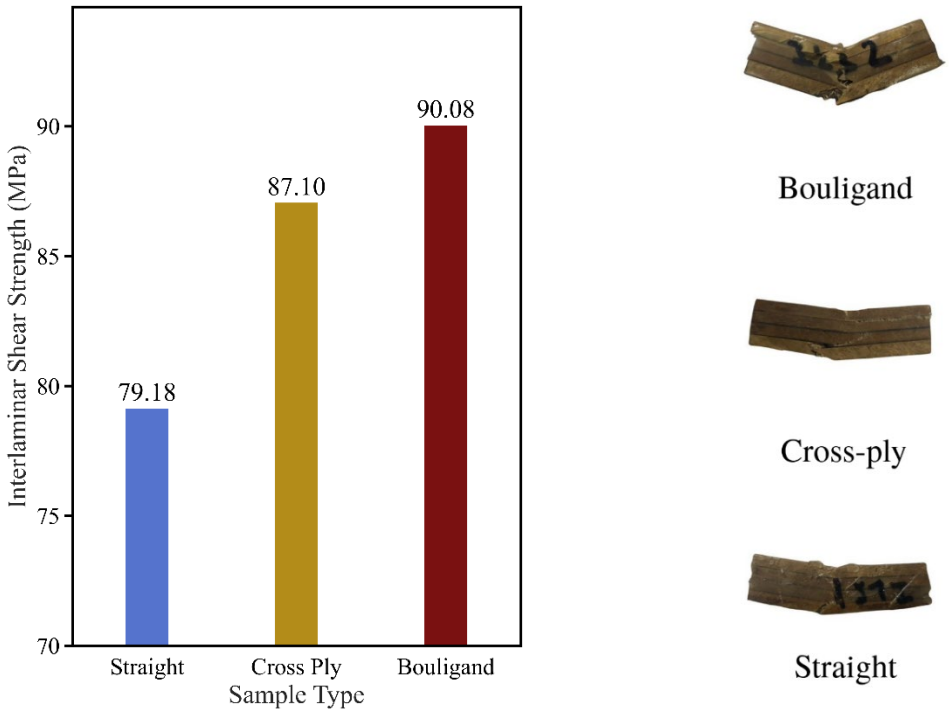

Figure 12: (a) Comparison of interlaminar shear strengths (ILSS) among different wood composite samples and (b) condition of the samples after ILSS testing

Interlaminar shear properties are excellent tools for quantitatively determining whether improvements in adhesion capacity can improve composite strength and impact resistance. Figure 9a shows the ILSS values of the different composite samples.

The failure modes observed in the test are mainly due to delamination of the top layer and shearing movement with the adjacent layer. The subsequent layers then fail either because of delamination or because of fiber breakage. Therefore, the adhesion capacity is the limiting factor in this test. The rotation of the fibers affects the stresses in different orientations in fiber-reinforced composites according to the literature [56]. Previous data are consistent with these results, as the straight (UD structure) sample has a value of 79.18 MPa, as shown in Figure 9a,

and the cross-ply structure has a value of 87.10 MPa. Since the Bouligand structure can create a more complex path for stress and crack propagation [1], it further enhances the adhesion strength to 90.08 MPa. Therefore, one of the underlying properties for the enhanced impact and flexural properties is the improvement in adhesion between layers. Nevertheless, since the jump in adhesion capacity is very minuscule, it is not the primary contributor.

4.2.7 Moisture Absorption Properties

An increase in the water resistance of the composite was observed during prolonged testing of the different samples. This is mainly due to the low moisture content of the epoxy [57]. The moisture absorption test results (Figure 10) revealed that all the samples exhibited an overall increase in mass over time, with an almost linear increase, except for the Bouligand and straight composite samples. This is expected, as while densification decreases the number of cavities inside wood [58], the epoxy on top of the ply blocks some pores, preventing water from being absorbed. After day 11, desorption occurred, which implies that the maximum capacity was reached; however, the moisture absorption rate increased with slight linearity for the composites after that, where it increased from 10.5 to 12 or nearly 12.

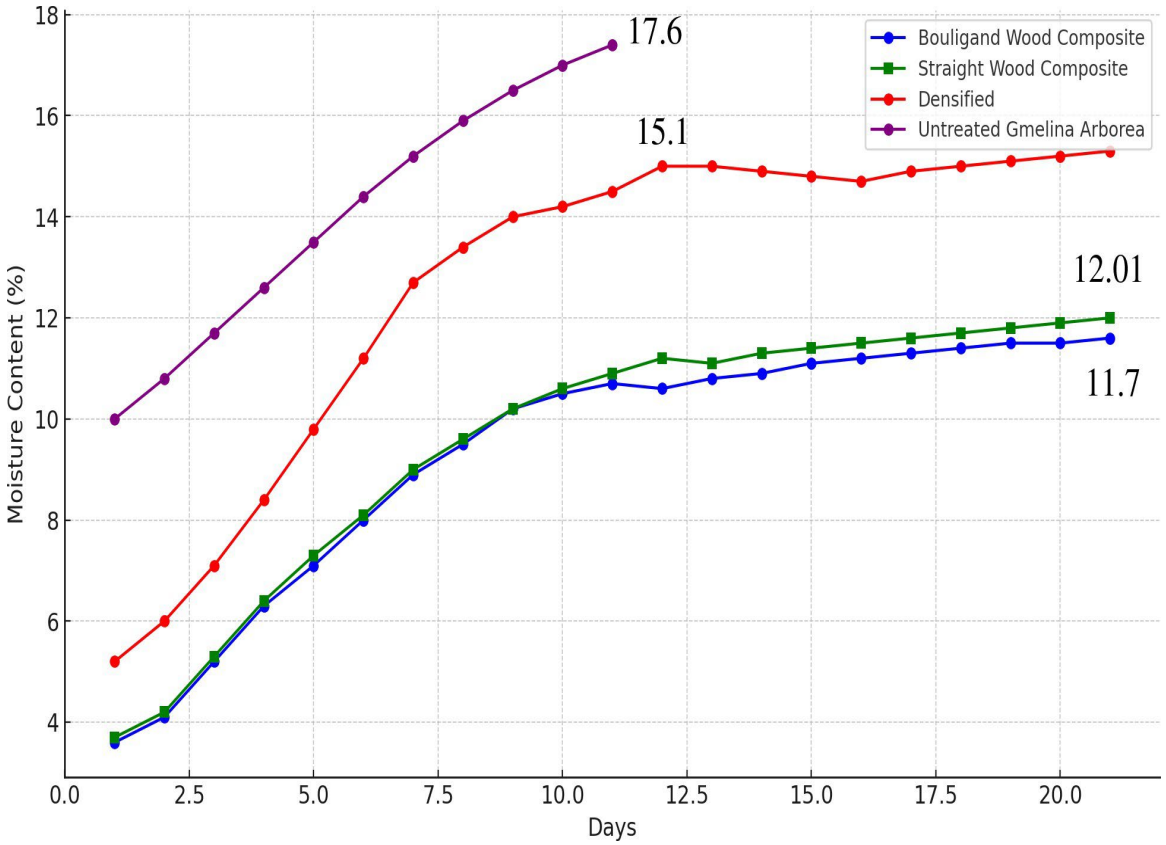

Figure 13: Moisture absorption properties over 21 days.

This shows no significant change in moisture absorption for the angular variation and stacking sequence of the composites. The Bouligand composite showed similar desorption after day 11, with a less steep decrease, but the rate increased as far as day 21. The untreated G. arborea sample presented a high rate of increase in moisture absorption until after day 11, when it was found to be rotten and unfit for further testing. This represents the failure of the wood to manage moisture, causing irreversible damage. In conclusion, while the Bouligand and straight composite had a hydrophobic nature, there was no significant difference in overall moisture absorption properties, with little to no improvement on either side.

4.3 Application of this study in the field of Mechanical engineering practice

The use of natural fiber composites in engineering has grown recently because of their benefits over traditional mineral fiber composites [61]. In Figure 12a and 12b, the relative performance of the Bouligand wood composite in terms of flexural and compressive strength is compared with that of other contemporary materials and potential application requirements. Specifically, Figure 12a shows the compressive strength relative to the density, whereas Figure 12b shows the flexural strength relative to the density.

The peak compression strength obtained for the composite was 61.54 MPa in the radial direction and 11.93 MPa in the longitudinal direction, indicating a nearly sixfold difference between the two orientations. Compression perpendicular to the grain is generally undesirable but is often unavoidable when timber structures are designed. This compression type commonly occurs in scenarios such as dowel-type joints, beam supports, and traditional longhouses construction [40]. In specific applications, the high deformation capacity of the Bouligand composite under such perpendicular grains can be purposefully utilized—for example, in cushioning materials and shock-absorbing components such as railway sleepers as a sustainable and lightweight alternative [62]. In contrast, when loaded radially, the Bouligand sample displayed a more positive outcome on the flexural side, with an ultimate strength of 198.22 MPa. The composite was very suitable for beam-related materials applications [60]. After further investigation of the fatigue life and damping properties of the material, it is suggested that this composite be utilized for structural appliances.

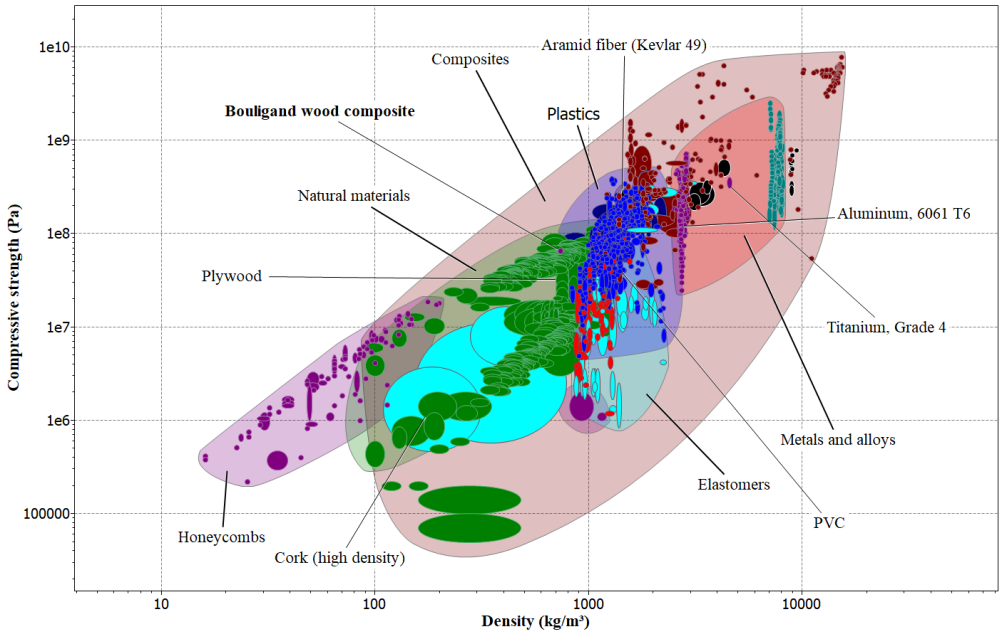

(a)

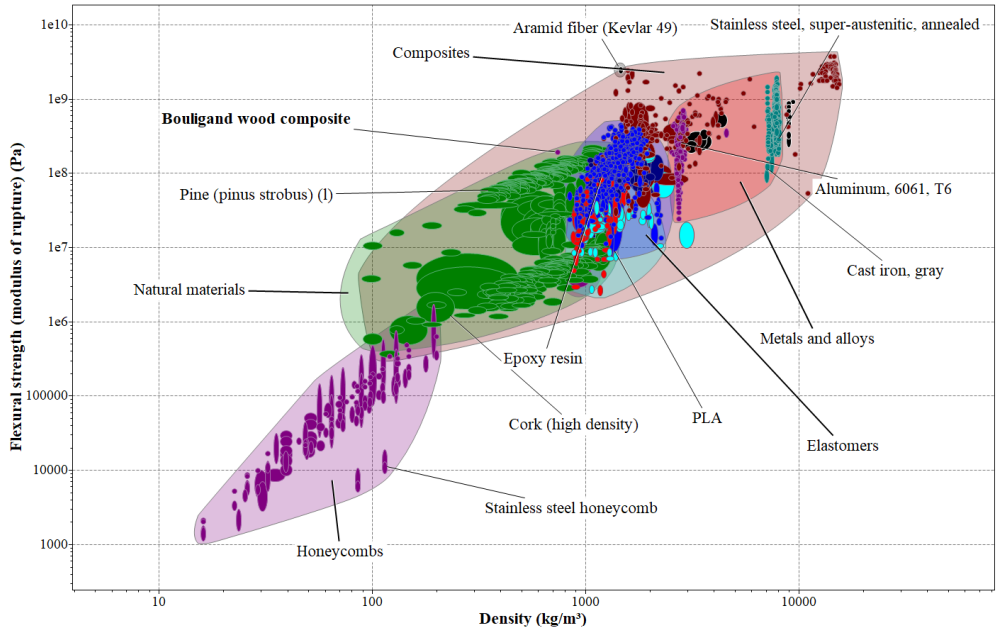

(b)

Figure 14: Ashby plots displaying (a) the compressive strength and (b) the flexural strength

From a performance and cost perspective, aluminum alloys and steel remain widely used due to their high yield strength, stiffness, and toughness, supported by mature and scalable processing technologies [63]. However, their relatively high densities—approximately 2.7 g/cm³ for aluminum and 7.7–8.0 g/cm³ for steel [64]—increase structural weight and associated

energy demands in applications such as transportation. In contrast, the Bouligand wood fiber composite developed in this study exhibits a density of only 0.738 g/cm³, offering a lightweight alternative to aluminum. Beyond weight reduction, its reinforcement phase is sourced from a renewable natural material, unlike aluminum, which requires energy-intensive extraction and processing. This combination of low density, mechanical efficiency, and renewable origin underscores the composite's potential as a sustainable alternative to conventional metallic materials.

4.4 Relation of this study for improving environmental benefits

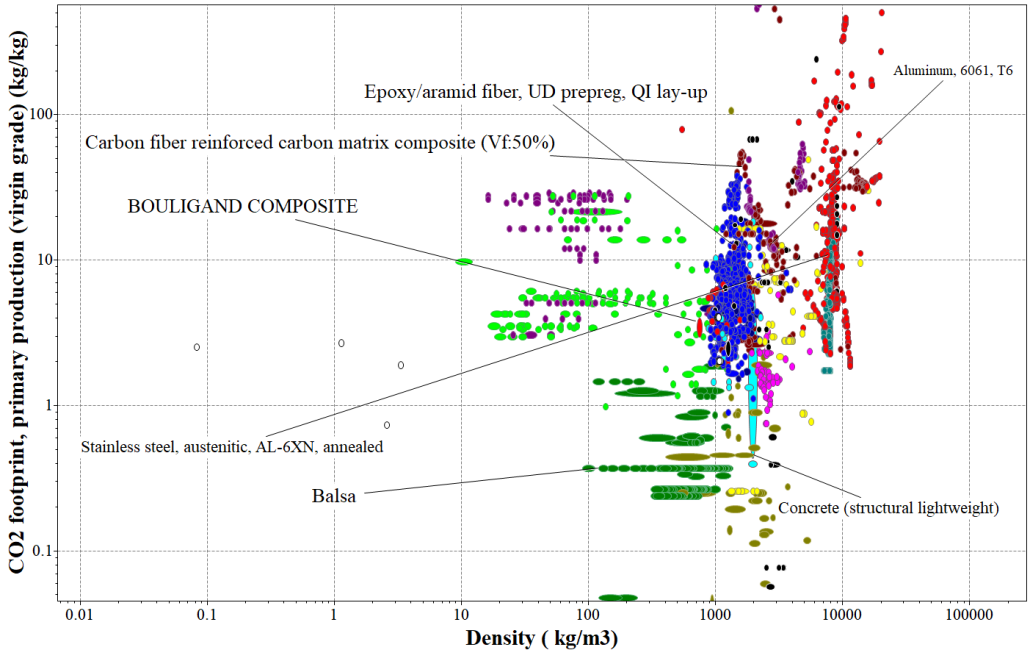

Figure 15: CO_2 footprint (production) of the Bouligand composite vs commonly used materials such as Kevlar 49, and Cork [59].

Figure 12c illustrates the variation in carbon footprint among engineering materials. Metals such as aluminum (6061, T6) cluster on the high-density, high-footprint side, with footprints exceeding 10 kg CO_2/kg, while stainless steels show lower values (~2–4 kg CO_2/kg) but remain density-intensive. In contrast, bio-based materials such as balsa occupy the low-density and low-footprint region, typically below 1 kg CO_2/kg, highlighting their environmental advantage despite lower structural performance. Synthetic fiber composites, including carbon fiber/epoxy and aramid/epoxy prepregs, appear in the mid-density but high-carbon-footprint region (10–100 kg CO_2/kg), reflecting the energy-intensive production of reinforcement fibers. By comparison, the Bouligand densified wood fiber composite situated in a more favorable part of the chart, combining moderate density with significantly reduced footprint. The overall trend emphasizes the potential of it as a sustainable alternative to conventional engineering materials.

4.5 Chapter conclusion

In conclusion, the results confirmed that the incorporation of a Bouligand-inspired helicoidal structure significantly enhanced the mechanical and environmental performance of the densified wood fiber composite. The optimized fiber rotation and layer configuration contributed to superior impact energy absorption, flexural strength, and interlaminar shear resistance compared to conventional stacking patterns. Microscopic analysis revealed that mechanisms such as fiber bridging, crack deflection, and improved fiber–matrix adhesion played a crucial role in energy dissipation and structural integrity. The reduced moisture uptake and favorable carbon footprint further validated the composite's potential as a lightweight and sustainable alternative to synthetic fiber materials. Collectively, the results demonstrate the success of the bioinspired design strategy and establish a solid foundation for the concluding chapter, which summarizes the overall findings, implications, and prospective applications of this research.

Chapter 5: Conclusion

5.1 Chapter Introduction

This chapter summarizes the key outcomes of the research and reflects on how the study objectives were achieved through experimental and analytical investigation. It consolidates the main findings related to the development, characterization, and performance evaluation of the Bouligand-inspired densified wood fiber composite. The chapter also highlights the significance of the bioinspired design approach, the material's mechanical and environmental advantages, and its potential applications in sustainable structural systems. Finally, it outlines the limitations of the current work and suggests possible directions for future research aimed at advancing the performance and scalability of natural fiber composites.

5.2 Conclusive Statements

The composite developed in this study is based on densified *Gmelina arborea* wood fibers, a renewable material that can reduce the need for synthetic or metallic alternatives. *Gmelina arborea* is a fast-growing hardwood species commonly cultivated in tropical regions. Its rapid growth and high biomass yield contribute to effective carbon sequestration, while its renewability and abundance reduce dependence on synthetic fibers with higher environmental costs [65]. With a low density of 0.738 g/cm³, the material is much lighter than aluminum (2.7 g/cm³) or steel (7.7–8.0 g/cm³), which can help lower energy use in transport and structural applications. The fabrication process relies on mechanical densification and slicing rather than energy-intensive melting or spinning, making it more efficient. Along with its ninefold improvement in impact resistance compared to untreated wood, the material offers durability that can extend service life and reduce replacement needs. By combining bioinspired design

with renewable resources, this composite points toward more practical and sustainable solutions for future engineering applications.

Mimicry of the internal structure of mantis shrimp has led to considerable improvements (10 times greater than that of the untreated wood and 3 times greater than that of the unidirectionally oriented composite in the Charpy test) and has also led to significant improvement in flexural strength (1.5 times greater than the strength of unidirectional fiber reinforcement) in terms of material strength compared with that of the regular configurations, which aligns with the goal of this study. The findings also suggest that biomimicry from a microstructure to a *mm* scale can still be helpful.

5.3 Recommendations for future work

The compression properties can be significantly improved by changing the plies' orientations and other reinforcing agents, such as nanoparticles. Another suggestion would be to study hybrid layups to enhance any properties further.

One limitation encountered during the fabrication process was the inability of the CNC machine to cut wood strips thinner than 2 mm. This constraint restricted the minimum achievable thickness for the layers. Additionally, no alternative equipment was available to produce thinner strips, limiting design flexibility and resulting in some material loss. Although epoxy provided strong bonding, its fossil origin limits sustainability. Developing natural or recyclable resin systems could enable fully green composites in future studies. However, some more limitations of the material also remain, one of which is that densified wood is not fireproof, and the fatigue life of the structure is yet to be determined.

5.4 Final Words

This research successfully demonstrated that adopting the Bouligand architecture in natural fiber composites can markedly improve mechanical performance, damage tolerance, and environmental sustainability. The developed densified wood composite, fabricated using *Gmelina Arborea* fibers and epoxy resin through controlled angular slicing and lamination, effectively replicated the helicoidal fiber alignment found in biological structures. Experimental analyses revealed that the Bouligand configuration exhibited a substantial enhancement in multiple mechanical domains compared to untreated wood and conventional stacking designs. Specifically, the impact strength increased nearly ninefold, while the flexural strength and modulus reached 198.22 MPa and 27.15 GPa, respectively, confirming superior load-bearing capacity and stiffness. The interlaminar shear strength was also notably higher, indicating improved interfacial adhesion due to the twisted fiber arrangement. Microscopic observations verified that mechanisms such as fiber pull-out, crack deflection, and ply rotation contributed significantly to energy dissipation and delayed fracture propagation. Moreover, the composite displayed reduced moisture absorption and a lower production-stage carbon footprint, reinforcing its environmental advantages. Overall, the findings validate that the Bouligand-inspired structural approach offers a scalable pathway for designing lightweight, renewable, and high-performance composites suitable for impact-resistant and structural applications in transportation and protective systems.

References

[1] N.A. Yaraghi, N. Guarín-Zapata, L.K. Grunenfelder, E. Hintsala, S. Bhowmick, J.M. Hiller, M. Betts, E.L. Principe, J. Jung, L. Sheppard, R. Wuhrer, J. McKittrick, P.D. Zavattieri, D. Kisailus, A Sinusoidally Architected Helicoidal Biocomposite, Advanced Materials 28 (2016) 6835–6844. https://doi.org/10.1002/adma.201600786.

[2] S.E. Naleway, M.M. Porter, J. McKittrick, M.A. Meyers, Structural Design Elements in Biological Materials: Application to Bioinspiration, Advanced Materials 27 (2015) 5455–5476. https://doi.org/10.1002/adma.201502403.

[3] U.G.K. Wegst, H. Bai, E. Saiz, A.P. Tomsia, R.O. Ritchie, Bioinspired structural materials, Nat Mater 14 (2015) 23–36. https://doi.org/10.1038/nmat4089.

[4] H. Ning, C. Monroe, S. Gibbons, B. Gaskey, P. Flater, A review of helicoidal composites: From natural to bio-inspired damage tolerant materials, International MaterialsReviews 69 (2024) 181–228. https://doi.org/10.1177/09506608241252498.

[5] J.C. Weaver, G.W. Milliron, A. Miserez, K. Evans-Lutterodt, S. Herrera, I. Gallana, W.J. Mershon, B. Swanson, P. Zavattieri, E. DiMasi, D. Kisailus, The Stomatopod Dactyl Club: A Formidable Damage-Tolerant Biological Hammer, Science (1979) 336 (2012) 1275–1280. https://doi.org/10.1126/science.1218764.

[6] V. Perricone, E. Sarmiento, A. Nguyen, N.C. Hughes, D. Kisailus, The convergent design evolution of multiscale biomineralized structures in extinct and extant organisms, Commun Mater 5 (2024) 227. https://doi.org/10.1038/s43246-024-00669-z.

[7] M.S. Aziz, A.Y. El Sherif, Biomimicry as an approach for bio-inspired structure with the aid of computation, Alexandria Engineering Journal 55 (2016) 707–714. https://doi.org/10.1016/J.AEJ.2015.10.015.

[8] N.S. Ha, G. Lu, A review of recent research on bio-inspired structures and materials for energy absorption applications, Compos B Eng 181 (2020) 107496.

https://doi.org/10.1016/J.COMPOSITESB.2019.107496.

[9] A. Sharma, N.K. Shukla, M.O. Belarbi, M. Abbas, A. Garg, L. Li, J. Bhutto, A. Bhatia, Bio-inspired nacre and helicoidal composites: From structure to mechanical applications, Thin-Walled Structures 192 (2023) 111146. https://doi.org/10.1016/J.TWS.2023.111146.

[10] D. Castelvecchi, Mantis shrimp have the world's fastest punch — here's how their limbs survive, Nature (2025). https://doi.org/10.1038/d41586-025-00386-8.

[11] A. Ghazlan, T. Ngo, P. Tan, Y.M. Xie, P. Tran, M. Donough, Inspiration from Nature's body armours – A review of biological and bioinspired composites, Compos B Eng 205 (2021). https://doi.org/10.1016/j.compositesb.2020.108513.

[12] S.-M. Chen, G.-Z. Wang, Y. Hou, X.-N. Yang, S.-C. Zhang, Z. Zhu, J. Li, H.-L. Gao, Y.-B. Zhu, H. Wu, S.-H. Yu, Hierarchical and reconfigurable interfibrous interface of bioinspired Bouligand structure enabled by moderate orderliness, Sci Adv 10 (2024). https://doi.org/10.1126/sciadv.adl1884.

[13] D. Nepal, S. Kang, K.M. Adstedt, K. Kanhaiya, M.R. Bockstaller, L.C. Brinson, M.J. Buehler, P. V. Coveney, K. Dayal, J.A. El-Awady, L.C. Henderson, D.L. Kaplan, S. Keten, N.A. Kotov, G.C. Schatz, S. Vignolini, F. Vollrath, Y. Wang, B.I. Yakobson, V. V. Tsukruk, H. Heinz, Hierarchically structured bioinspired nanocomposites, Nat Mater 22 (2023) 18–35. https://doi.org/10.1038/s41563-022-01384-1.

[14] A. Kumar, T. Jyske, M. Petrič, Delignified Wood from Understanding the Hierarchically Aligned Cellulosic Structures to Creating Novel Functional Materials: A Review, Adv Sustain Syst 5 (2021). https://doi.org/10.1002/adsu.202000251.

[15] A. Mishra, F. Humpenöder, G. Churkina, C.P.O. Reyer, F. Beier, B.L. Bodirsky, H.J. Schellnhuber, H. Lotze-Campen, A. Popp, Land use change and carbon emissions of a transformation to timber cities, Nat Commun 13 (2022) 4889. https://doi.org/10.1038/s41467-022-32244-w.

[16] C. Chen, Y. Kuang, S. Zhu, I. Burgert, T. Keplinger, A. Gong, T. Li, L. Berglund,

S.J. Eichhorn, L. Hu, Structure–property–function relationships of natural and engineered wood, Nat Rev Mater 5 (2020) 642–666. https://doi.org/10.1038/s41578-020-0195-z.

[17] S. Namari, L. Drosky, B. Pudlitz, P. Haller, A. Sotayo, D. Bradley, S. Mehra, C. O'Ceallaigh, A.M. Harte, I. El-Houjeyri, M. Oudjene, Z. Guan, Mechanical properties of compressed wood, Constr Build Mater 301 (2021) 124269. https://doi.org/10.1016/j.conbuildmat.2021.124269.

[18] J. Song, C. Chen, S. Zhu, M. Zhu, J. Dai, U. Ray, Y. Li, Y. Kuang, Y. Li, N. Quispe, Y. Yao, A. Gong, U.H. Leiste, H.A. Bruck, J.Y. Zhu, A. Vellore, H. Li, M.L. Minus, Z. Jia, A. Martini, T. Li, L. Hu, Processing bulk natural wood into a high-performance structural material, Nature 554 (2018) 224–228. https://doi.org/10.1038/nature25476.

[19] J. Brauns, K. Rocens, Modification of Wood: Mechanical Properties and Application, Encyclopedia of Materials: Science and Technology (2007) 1–9. https://doi.org/10.1016/B978-008043152-9.02174-6.

[20] L. Lin, F. Fu, L. Qin, Cellulose fiber-based high strength composites, Advanced High Strength Natural Fibre Composites in Construction (2017) 179–203. https://doi.org/10.1016/B978-0-08-100411-1.00007-8.

[21] P. Mania, M. Wróblewski, A. Wójciak, E. Roszyk, W. Moliński, Hardness of Densified Wood in Relation to Changed Chemical Composition, Forests 11 (2020) 506. https://doi.org/10.3390/f11050506.

[22] A. Sikora, M. Gaff, A. Kumar Sethy, N. Fantuzzi, P. Horáček, Bending work of laminated materials based on densified wood and reinforcing components, Compos Struct 274 (2021). https://doi.org/10.1016/j.compstruct.2021.114319.

[23] D.B. Dittenber, H.V.S. GangaRao, Critical review of recent publications on use of natural composites in infrastructure, Compos Part A Appl Sci Manuf 43 (2012) 1419–1429. https://doi.org/10.1016/j.compositesa.2011.11.019.

[24] A.K. Mohanty, M. Misra, L.T. Drzal, Surface modifications of natural fibers and performance of the resulting biocomposites: An overview, Compos Interfaces 8

(2001) 313–343. https://doi.org/10.1163/156855401753255422.

[25] K. Gruebler, D. Thomson, N. Petrinic, M.R. Wisnom, S.R. Hallett, Fibre reinforcement and stacking sequence influence on the through-thickness compression behaviour of polymer composites, Compos Struct 319 (2023) 117160. https://doi.org/10.1016/j.compstruct.2023.117160.

[26] P.R. Govindarajan, R. Shanmugavel, K. Subramanian, S. Palanisamy, C. Santulli, C. Fragassa, Effect of Stacking Sequence on Mechanical and Water Absorption Characteristics of Jute/Banana/Basalt Fabric Aluminium Fibre Laminates With Diamond Microexpanded Mesh, Int J Polym Sci 2024 (2024). https://doi.org/10.1155/2024/3835788.

[27] Y. Xu, D. Feng, Enhancing impact resistance of fiber-reinforced polymer composites through bio-inspired helicoidal structures: A review, Polym Compos 46 (2025) 5823–5856. https://doi.org/10.1002/pc.29352.

[28] B. Natarajan, J.W. Gilman, Bioinspired Bouligand cellulose nanocrystal composites: a review of mechanical properties, Philosophical Transactions of the Royal Society A: Mathematical, Physical and Engineering Sciences 376 (2018) 20170050. https://doi.org/10.1098/rsta.2017.0050.

[29] K. Wu, Z. Song, S. Zhang, Y. Ni, S. Cai, X. Gong, L. He, S.-H. Yu, Discontinuous fibrous Bouligand architecture enabling formidable fracture resistance with crack orientation insensitivity, Proceedings of the National Academy of Sciences 117 (2020) 15465–15472. https://doi.org/10.1073/pnas.2000639117.

[30] P. Cui, J. Chen, K. Fu, J. Deng, T. Sun, K. Chen, P. Yin, Bioinspired Bouligand-Structured Cellulose Nanocrystals/Poly(vinyl alcohol) Composite Hydrogel for Enhanced Impact Resistance, ACS Appl Mater Interfaces 16 (2024) 53022–53032. https://doi.org/10.1021/acsami.4c13264.

[31] L.-F. Yang, X.-S. Zhang, X.-Y. Huang, J. Chen, Y.-F. Mao, J. Wang, W. Huang, F.-D. Nie, J. Wang, Biomimetic Bouligand structure assisted mechanical enhancement of highly particle-filled polymer composites, Addit Manuf 100 (2025) 104666. https://doi.org/10.1016/j.addma.2025.104666.

[32] A. Prihar, S. Gupta, H.S. Esmaeeli, R. Moini, Tough double-bouligand architected concrete enabled by robotic additive manufacturing, Nat Commun 15 (2024) 7498. https://doi.org/10.1038/s41467-024-51640-y.

[33] M. Broda, S. Curling, M. Frankowski, The effect of the drying method on the cell wall structure and sorption properties of waterlogged archaeological wood, Wood Sci Technol 55 (2021) 971–989. https://doi.org/10.1007/s00226-021-01294-6.

[34] P. Mania, C. Kupfernagel, S. Curling, Densification of Delignified Wood: Influence of Chemical Composition on Wood Density, Compressive Strength, and Hardness of Eurasian Aspen and Scots Pine, Forests 15 (2024). https://doi.org/10.3390/f15060892.

[35] S.Y. Ha, J.Y. Jung, H.C. Kim, W.S. Lim, J.-K. Yang, Low-temperature and low-concentration sodium hydroxide pretreatment for enhanced enzyme hydrolysis rate from Quercus variabilis Blume, Bioresources 19 (2024) 2592–2608. https://bioresources.cnr.ncsu.edu/resources/low-temperature-and-low-concentration-sodium-hydroxide-pretreatment-for-enhanced-enzyme-hydrolysis-rate-from-quercus-variabilis-blume/.

[36] J. Li, C. Chen, J.Y. Zhu, A.J. Ragauskas, L. Hu, In Situ Wood Delignification toward Sustainable Applications, Acc Mater Res 2 (2021) 606–620. https://doi.org/10.1021/accountsmr.1c00075.

[37] D. Schieppati, N.A. Patience, F. Galli, P. Dal, I. Seck, G.S. Patience, D. Fuoco, X. Banquy, D.C. Boffito, Chemical and Biological Delignification of Biomass: A Review, Ind Eng Chem Res 62 (2023) 12757–12794. https://doi.org/10.1021/acs.iecr.3c01231.

[38] C.H. Park, W.S. Lee, Y.E. Yoo, E.J. Kim, A study on fiber orientation in the compression molding of fiber reinforced polymer composite material, J Mater Process Technol 111 (2001) 233–239. https://doi.org/10.1016/S0924-0136(01)00523-4.

[39] C.A. Schneider, W.S. Rasband, K.W. Eliceiri, NIH Image to ImageJ: 25 years of image analysis, Nat Methods 9 (2012) 671–675.

https://doi.org/10.1038/nmeth.2089.

[40] G. Wu, Y. Shen, F. Fu, J. Guo, H. Ren, Study of the Mechanical Properties of Wood under Transverse Compression Using Monto Carlo Simulation-Based Stochastic FE Analysis, Forests 13 (2021) 32. https://doi.org/10.3390/f13010032.

[41] Y. Miyoshi, K. Kojiro, Y. Furuta, Effects of density and anatomical feature on mechanical properties of various wood species in lateral tension, Journal of Wood Science 64 (2018) 509–514. https://doi.org/10.1007/s10086-018-1730-z.

[42] S. Mortazavian, A. Fatemi, Effects of fiber orientation and anisotropy on tensile strength and elastic modulus of short fiber reinforced polymer composites, Compos B Eng 72 (2015) 116–129. https://doi.org/10.1016/j.compositesb.2014.11.041.

[43] D. Guo, X. Shen, F. Fu, S. Yang, G. Li, F. Chu, Improving physical properties of wood–polymer composites by building stable interface structure between swelled cell walls and hydrophobic polymer, Wood Sci Technol 55 (2021) 1401–1417. https://doi.org/10.1007/s00226-021-01317-2.

[44] D. Guo, N. Guo, F. Fu, S. Yang, G. Li, F. Chu, Preparation and mechanical failure analysis of wood-epoxy polymer composites with excellent mechanical performances, Compos B Eng 235 (2022). https://doi.org/10.1016/j.compositesb.2022.109748.

[45] R. GANESAN, Experimental characterization of interlaminar shear strength, in: Delamination Behaviour of Composites, Elsevier, 2008: pp. 117–137. https://doi.org/10.1533/9781845694821.1.117.

[46] Md.T.A. Ansari, K.K. Singh, Md.S. Azam, Effect of Ply Stacking and Fiber Volume Fraction on ILSS of Woven GFRP Laminates, in: 2020: pp. 561–568. https://doi.org/10.1007/978-981-15-2647-3_51.

[47] J.A. Bennett, R.J. Young, The effect of fibre-matrix adhesion upon crack bridging in fibre reinforced composites, n.d.

[48] W.J. Cantwell, J. Morton, The impact resistance of composite materials — a review, Composites 22 (1991) 347–362. https://doi.org/10.1016/0010-4361(91)90549-V.

[49] D. Hull, T.W. Clyne, An Introduction to Composite Materials, 2nd ed., Cambridge University Press, 1996. https://doi.org/10.1017/CBO9781139170130.

[50] A.M. Asan, M.O. Kaman, S. Dag, S. Erdem, K. Turan, Effects of translaminar edge crack and fiber angle on fracture toughness and crack propagation behaviors of laminated carbon fiber composites, International Journal of Materials Research 115 (2024) 446–462. https://doi.org/10.1515/ijmr-2023-0317.

[51] L. Schöttl, P. Kolb, W. V. Liebig, K.A. Weidenmann, K. Inal, P. Elsner, Crack characterization of discontinuous fiber-reinforced composites by using micro-computed tomography: Cyclic in-situ testing, crack segmentation and crack volume fraction, Composites Communications 21 (2020) 100384. https://doi.org/10.1016/j.coco.2020.100384.

[52] W. Hu, Y. Liu, S. Li, Characterizing Mode I Fracture Behaviors of Wood Using Compact Tension in Selected System Crack Propagation, Forests 12 (2021) 1369. https://doi.org/10.3390/f12101369.

[53] S. Chandrasekaran, N. Sato, F. Tölle, R. Mülhaupt, B. Fiedler, K. Schulte, Fracture toughness and failure mechanism of graphene based epoxy composites, Compos Sci Technol 97 (2014) 90–99. https://doi.org/10.1016/j.compscitech.2014.03.014.

[54] S.A. Mirsalehi, A.A. Youzbashi, A. Sazgar, Enhancement of out-of-plane mechanical properties of carbon fiber reinforced epoxy resin composite by incorporating the multi-walled carbon nanotubes, SN Appl Sci 3 (2021) 630. https://doi.org/10.1007/s42452-021-04624-2.

[55] M. Hartwig-Nair, S. Florisson, M. Wohlert, E.K. Gamstedt, Characterisation of hygroelastic properties of compression and opposite wood found in branches of Norway spruce, Wood Sci Technol 58 (2024) 887–906. https://doi.org/10.1007/s00226-024-01548-z.

[56] F. Javanshour, A. Prapavesis, T. Pärnänen, O. Orell, M.C. Lessa Belone, R.K. Layek, M. Kanerva, P. Kallio, A.W. Van Vuure, E. Sarlin, Modulating impact resistance of flax epoxy composites with thermoplastic interfacial toughening, Compos Part A Appl Sci Manuf 150 (2021) 106628.

https://doi.org/10.1016/j.compositesa.2021.106628.

[57] O. Faruk, A.K. Bledzki, H.-P. Fink, M. Sain, Biocomposites reinforced with natural fibers: 2000–2010, Prog Polym Sci 37 (2012) 1552–1596. https://doi.org/10.1016/j.progpolymsci.2012.04.003.

[58] J. Wang, Y. Chai, J. Liu, J.Y. Zhu, The Viscoelastic and Hygroscopicity Behavior of Delignified and Densified Poplar Wood, Forests 14 (2023) 1721. https://doi.org/10.3390/f14091721.

[59] Ansys, *Granta Selector*, version 2023, Ansys Inc. (2023).

[60] L. Yao, L. Ji, Z. Wang, J. Liu, Bending Performance of Plantation Teakwood and Its Mechanism Based on Radial and Tangential Directions, Forests 15 (2024) 2203. https://doi.org/10.3390/f15122203.

[61] R. Sundaram, B. Vinayagam, K. Chandrasekaran, S. Rajendran, A. Kumar, S. Ramakrishna, Significance of ballistic parameters and nanohybridization in the development of textile-based body armor: A review, Int J Impact Eng 180 (2023) 104700. https://doi.org/10.1016/j.ijimpeng.2023.104700.

[62] C. Esveld, Modern Railway Track, 2nd ed., MRT-Productions, Delft, The Netherlands, 2001.

[63] M.R. Mansor, A.H. Nurfaizey, N. Tamaldin, M.N.A. Nordin, Natural fiber polymer composites, in: Biomass, Biopolymer-Based Materials, and Bioenergy, Elsevier, 2019: pp. 203–224. https://doi.org/10.1016/B978-0-08-102426-3.00011-4.

[64] S.M. Arnold, D. Cebon, M. Ashby, Materials selection for aerospace, in: A. Mouritz (Ed.), Introduction to Aerospace Materials, Woodhead Publishing Limited, Cambridge, UK, 2012: pp. 569–600.